Conceptus-induced interferon tau-dependent gene expression in bovine endometrial epithelial and stroma fibroblast cells

Heather L. Baldwin[1], Lindsay F. Grose[1], Gilles Charpigny[2], Susanta K. Behura[3], I. Martin Sheldon[4], James G. Cronin[4], Patrick Lonergan[5], Thomas E. Spencer[3], Daniel J. Mathew[6]

[1]Davis College of Agriculture, Natural Resources and Design, Division of Animal and Nutritional Sciences, West Virginia University, Morgantown, WV, USA

[2]INRA, Biologie du Développement et Reproduction, 78350, Jouy en Josas, France

[3]Division of Animal Sciences, University of Missouri, Columbia, MO, USA

[4]Swansea University Medical School, Swansea University, Swansea, SA2 8PP, UK

[5]School of Agriculture and Food Science, University College Dublin, Belfield, Dublin, Ireland

[6]Department of Animal Science, The University of Tennessee, Knoxville, TN

Corresponding author: Daniel J. Mathew

Short title: IFNT and endometrial cell transcriptome

Word Count:

Keywords: Interferon-tau, endometrium, transcriptome, embryo, 3D cell culture

Abstract

Conceptus-derived interferon-tau (IFNT) is the maternal recognition of pregnancy (MRP) signal in ruminants. It suppresses the endometrial luteolytic mechanism, thus maintaining the corpus luteum and progesterone secretion in support of gestation. The endometrium largely consists of epithelial and stroma fibroblast cells that are stimulated by IFNT to express interferon-stimulated genes (ISGs). The ISGs are believed to have essential functions related to the establishment of pregnancy in ruminants and independent of maternal recognition of pregnancy; however, endometrial epithelial and fibroblast cell type-specific expression of the ISGs is largely unknown. The objective of this study was to gain a better understanding of endometrial epithelial and fibroblast cell type-specific expression of ISGs in response to IFNT. Bovine endometrial epithelial cells were cultured in transwell inserts above bovine endometrial fibroblast cells for 6 h in medium alone (n=4) or in the presence of 100 ng/mL of recombinant ovine IFNT (n=3). Total RNA was extracted from both cell types and the transcriptomes were assayed by RNA Sequencing. Select transcripts were validated by RT-qPCR. Interferon-tau differentially regulated 663 and 80 genes (DEGs) in epithelial and fibroblast cells, respectively ($P \leq 0.001$; FDR $P \leq 0.05$). To focus on genes biologically relevant to early pregnancy in cattle, data were then compared to a list of 369 DEGs recently identified in intact bovine endometrium in

response to elongating bovine conceptuses and recombinant IFNT. Bovine endometrial epithelial and fibroblast cells shared 223 and 70 DEGs in common with the list of 369 endometrial DEGs. Many of the DEGs identified in the epithelial and fibroblast cells in common with the endometrium were well known ISGs including *ISG15*, *MX1*, *MX2*, and *OAS2*. DEGs identified in the epithelial but not stroma fibroblast cells, yet, in common with the endometrium included a number of IRF molecules (*IRF1*, *IRF2*, *IRF3* and *IRF8*), mitochondria SLC transporters (*SLC25A19*, *SLC25A28* and *SLC25A30*), and a ghrelin receptor (*GHSR*). The gene *ZC3HAV1*, which was also recently found to be up-regulated in intact bovine endometrium in response to the conceptus, was only up-regulated in the fibroblast cells. Gene ontology analysis identified the type-1 interferon signaling pathway and defense response to virus as the top two biological processes associated with the epithelial and fibroblast cells DEGs in common with the endometrial DEGs. This study identified bovine endometrial epithelial and stroma fibroblast cell type-specific expression of ISGs in response to IFNT, a type I IFN and the MRP signal in ruminants.

Introduction

Early embryonic mortality, defined as the death or loss of embryos within the first 27 days of gestation in cattle, is a major component of reproductive failure [1]. While the causes of early embryonic mortality are multifaceted and complex [2], inadequate or asynchronous paracrine communication between the conceptus and endometrium, particularly during maternal recognition of pregnancy (MRP), make a significant contribution to this loss [3-6]. Approximately two weeks after fertilization in cattle, the conceptus (embryo and

68 extraembryonic tissues) will undergo a major morphological transformation, changing from a
69 spherical blastocyst to a long tubular and then filamentous structure. The process, referred to
70 as elongation, is coincident with conceptus secretion of interferon tau (IFNT), the MRP signal in
71 ruminants. A type I interferon, IFNT stimulates uterine cells to express interferon-stimulated
72 genes (ISGs) and disrupts the endometrial luteolytic mechanism by blocking pulsatile secretion
73 of prostaglandin F2 alpha ($PGF_{2\alpha}$) from the uterine surface epithelium, thereby maintaining
74 progesterone (P4) secretion by the corpus luteum (CL) [7-9]. Although *in vitro* produced bovine
75 blastocysts express *IFNT* as early as Day 7 of development, the critical period for conceptus IFNT
76 secretion is between Days 16 and 17 of gestation [10-12].
77 Bovine endometrium consists of aglandular (caruncular) and glandular (intercaruncular)
78 regions. Within the intercaruncular regions, the endometrium is highly secretory and consists
79 largely of stroma fibroblast (SF) cells and luminal epithelial (LE) and glandular epithelial (GE)
80 cells. The uterine LE cells are separated from the underlying SF by a basement membrane and
81 are continuous with the GE that penetrate down into the stroma forming uterine glands [13].
82 Within the stroma, the uterine glands branch repeatedly, maximizing the secretion of
83 endometrial histotroph by increasing epithelial surface area. A complex mixture of proteins,
84 amino acids, steroids, prostaglandins, ions as well as exosomes, and histotroph are secreted in
85 response to ovarian P4 [14, 15] and conceptus secretory factors, including IFNT, ultimately
86 promoting the development of the conceptus [16-18].
87 In cattle and sheep, IFNT binds the type I interferon alpha receptor (IFNAR) in the
88 uterine epithelia and SF, activating the janus associated kinase-signal transducer and activator
89 of transcription (Jak-STAT) signaling pathway [19, 20]. In this way, IFNT stimulates expression of

so-called “classical” ISGs in the SF [21]. In the uterine surface epithelia, however, IFNT is hypothesized to stimulate activity of a classical ISG inhibitor, interferon regulatory factor 2 (IRF2), as well as mitogen activated protein kinases (MAPK) and phosphatidyl inositol 3 kinase (PI3K) signaling pathways resulting in expression of “non-classical” ISGs [19, 22, 23]. Many IFNT stimulated, endometrial cell type-specific, classical and non-classical ISGs have been identified in sheep with less information available for cattle [16, 24]. Further, transcriptomic and *in situ* hybridization (ISH) studies of the endometrium during early pregnancy in cattle and sheep have exposed species-specific differences in terms of endometrial cell type-specific expression of ISGs [16]. Regardless, classical and non-classical ISGs are hypothesized to have important functions during early pregnancy related to histotroph composition, maternal immune tolerance to the conceptus, endometrial architecture changes for uterine receptivity, and vascular remodeling for maternal-fetal nutrient and waste exchange [25-29]. Undoubtedly, these physiological processes are highly dependent on endometrial cell type expression of ISGs.

We recently identified conceptus-induced, IFNT-dependent (CiTd) and independent (CiTi) differentially expressed genes (DEGs) in bovine endometrium following culture of mid-luteal phase endometrial explants in the absence or presence of recombinant ovine IFNT or elongating Day 15 bovine conceptuses [30]. Overall, 369 CiTd endometrial DEGs were identified during the study including classical and non-classical ISGs previously identified in cattle or sheep as well as newly discovered ISGs in cattle. The endometrial cell types responsible for expression of the DEGs, however, were not identified.

Building on those findings, here we attempted to identify bovine CiTd endometrial DEGs expressed within the bovine endometrial epithelia and SF. To do this, we isolated bovine

endometrial epithelium and SF from mid-luteal phase endometrium and treated the cells with recombinant ovine IFNT in a three-dimensional (3D) cell culture system. We then conducted RNA Sequencing (RNA-Seq) and Real Time-quantitative Polymerase Chain Reaction (RT-qPCR) on the endometrial epithelial and SF mRNAs. To better focus on physiologically relevant pathways, the epithelial and SF RNA-Seq data were then compared to the list of bovine CiTd endometrial DEGs recently published by Mathew et al. [30]. We hypothesized that differences in IFNT-stimulated endometrial epithelium and SF gene expression would reflect important cell type-specific activities during conceptus elongation and maternal recognition of pregnancy in cattle. Importantly, the information will increase our understanding of conceptus-maternal crosstalk at a critical period in embryonic development.

Materials and Methods

Bovine Endometrial Cell Isolation and Culture

Reproductive tracts from continental breed beef heifers were collected from a local abattoir within approximately 20 min of slaughter. The tracts were chosen based on appearance of a mid-luteal phase CL (Days 11 to 17 of the estrous cycle; Stage III) as described by Ireland et al. [31] and the absence of pregnancy or infection. The reproductive tracts were transported to the laboratory on ice (approximately 30 min drive) and immediately rinsed with Dulbecco's phosphate-buffered saline (DPBS; Gibco, ThermoFisher Scientific) at R.T. The broad ligament, oviduct, and ovary were dissected away from the uterine horn ipsilateral to the CL before removing the entire uterine horn from the remaining reproductive tract at the uterine bifurcation. The uterine horn was pinched closed, washed with DPBS (R.T.), and sprayed with

70% ethanol before laid on ethanol soaked (70%) paper towel within a dissecting tray. Using sterile scissors, the uterine horns were dissected open along the anti-mesometrial side to the utero-tubule junction. The endometrium was then observed for the absence of a conceptus, infection related puss, or discoloration and then washed with DPBS (R.T.) containing 1% antibiotic-antimycotic (ABAM; Gibco, ThermoFisher Scientific).

Bovine endometrial epithelial and SF cells were isolated as previously described but with modifications [32-34]. Briefly, intercaruncular endometrial strips were dissected away from the myometrium and washed in Hank's Balanced Salt Solution (HBSS; Gibco, ThermoFisher Scientific) (R.T.) containing 1% ABAM before dissected into 3 mm^3 pieces and enzymatically digested in 30 mL of HBSS containing collagenase type II (0.5 mg/mL; Sigma-Aldrich), bovine serum albumin (BSA, 1 mg/mL; Sigma-Aldrich), trypsin (2.5 BAEE units/mL; Sigma-Aldrich) and DNase 1 (0.1 mg/mL; Sigma-Aldrich) for 1 h in a shaking water bath at 38.8°C. The digested solution was then filtered through a 100 µm cell strainer positioned over a 40 µm cell strainer (Corning) into a 50 mL conical tube (Falcon) containing HBSS (10% fetal bovine serum, FBS; Sigma-Aldrich). To establish the SF cell cultures, the filtered endometrial cells were processed through a series of two centrifugations (700 x g for 7 min at R.T.) and washes before re-suspended in 45 mL of Roswell Park Memorial Institute (RPMI) 1640 medium (Gibco, ThermoFisher Scientific) containing 10% FBS and 1% ABAM (cell culture media throughout). The re-suspended cells were then plated (15 mL) into T75 flasks (Greiner Bio-One). To establish endometrial epithelial cell cultures and collect sheets of LE and GE, the 40 µm cell strainer used during the initial filtration process was back washed with cell culture media into a conical tube and immediately plated (15 mL) into T75 flasks. The SF and epithelial cells were cultured at

38.8°C in 5.0% CO_2 and humidified air (cell culture conditions throughout). SF and epithelial cell cultures were washed with DPBS (1% ABAM) and new cell culture media was added 18 and 48 h post-plating, respectively.

Endometrial SF and epithelial cell cultures were purified within a week due to their proliferation characteristics and differential adhesive properties. Once the SF cultures were approximately 80-90% confluent, the cells were detached from the plate and passaged by incubating the cells with Accutase (Sigma) for approximately 5 min. Contaminating epithelial cells remained attached to the original T75 plates due to their greater adhesive properties and discarded. For the epithelial cell cultures, contaminating fibroblasts were removed similar to SF cell passage, by adding Accutase to the epithelial cultures and then washing the T75 with DPBS (1% ABAM) to remove the suspended fibroblasts. New culture media was then added back to the T75 containing the epithelial cells. To detach and pass the epithelial cells, Accutase was added to the cultures for approximately 15-20 min. Primary cultures of SF and epithelial cells were passaged approximately 8 and 3 times, respectively, before being utilized for staining and 3D cell culture.

Immunocytochemistry (ICC) of Endometrial Cell Monocultures

To assess the purity of the SF and epithelial cell monocultures before 3D culture, a dual immunofluorescent staining technique for vimentin and cytokeratin, mesenchyme and epithelial cell proteins, respectively, was utilized. Briefly, SF and epithelial cell cultures were plated (1 mL; 1 X 10^5 cells/mL) into wells of a 24 well plate (TPP, Sigma) coated with a 0.1% gelatin (Sigma) in distilled water. When approximately 80-90% confluent, the cell cultures were

178 fixed in the plate for 20 min at R.T. with a 2% neutral buffered formalin (NBF; Sigma) in DPBS
179 (Sigma) solution, permeated for 10 min at R.T. with a 0.1% Triton X-100 (TX-100; Sigma) in DPBS
180 solution and blocked for 45 min at 37°C with a 10% goat serum (Sigma) in DPBS solution
181 containing 0.1% Tween-20 (Sigma; DPBS-T). After, the cells were washed with DPBS-T and
182 incubated overnight at 4°C with 500 µL of a primary antibody solution consisting of 52.5 µg/mL
183 of mouse monoclonal anti-cytokeratin IgG antibody (C2562, Sigma) and 1:400 dilution
184 (approximately 2.5-7.5 µg total protein from culture supernatant/mL) of rabbit monoclonal
185 anti-vimentin IgG antibody (SP20, ab16700; Abcam) in DPBS-T containing 1.5% goat serum
186 (Sigma). Fixed epithelial and fibroblast cell cultures were also incubated with 500 µL of a
187 primary antibody control solution consisting of 52.5 µg/mL mouse IgG (I8765; Sigma) and 1:400
188 dilution of rabbit serum (R9133; Sigma; approximately 30-36.2 µg/mL of IgG) in DPBS-T
189 containing 1.5% goat serum.
190 The next day the fixed cells were washed with DPBS-T and incubated at R.T. in the dark
191 for 1 h with a secondary antibody solution consisting of goat-anti-mouse IgG antibody
192 conjugated to Alexa Fluor 488 (A-11001; Thermo Scientific) and goat anti-rabbit IgG antibody
193 conjugated to Alexa Fluor 594 (A-11037; Thermo Scientific) in DPBS-T containing 1.5% goat
194 serum (Sigma). Cells were washed with DPBS-T and incubated for 5 min in the dark with 1
195 µg/mL of Hoechst in DPBS-T. After a final wash with DPBS-T, images were taken of the cells with
196 a D2H camera (Nikon) and Eclipse TE-2000-S (Nikon) inverted microscope able to detect
197 fluorescence. Fluorescent and grayscale brightfield images of the SF and epithelial cells were
198 merged using the merge channel feature in the NIH Image J computer program. Staining for
199 cytokeratin was detected within primary epithelial cell cultures but not SF cultures (Figure 1)

indicating the two cell populations were separated. Vimentin was detected within both cell types. Vimentin expression in isolated bovine endometrial epithelial cells has been reported and has been attributed to loss off cell to cell contact during isolation resulting in a limited epithelial to mesenchyme transition [35].

Collection of Pregnant Ovine Uterine Flush Fluid

To test the responsiveness of bovine endometrial cells in the 3D cell culture system prior to treatment with recombinant ovine IFNT, 3D cultures were treated with Day 14 pregnant ovine uterine flush fluid (UFF) collected during a previous study. Naturally produced ovine conceptus IFNT within the UFF should induce endometrial epithelial cell and SF ISG expression. All procedures were in compliance with the Guide for the Care and Use of Agriculture Animals in Research and Teaching and approved by the West Virginia University Institutional Animal Care and Use Committee. Briefly, reproductive cycles of post-pubertal Texel ewes were synchronized after 5 days of vaginal absorption of P4 via controlled internal drug release (0.3 g P4; EAZI-BREED CIDR) [36]. One day after CIDR removal ewes were bred by a Texel ram fitted with a mounting harness. Fourteen days after mating ewes were euthanized and the reproductive tract was collected. The uterine horns were flushed with 20 mL of ice-cold DPBS and uterine contents were collected into a petri dish. Pregnancy was confirmed if an elongated conceptus was flushed from the uterus. The UFF was centrifuged for 15 min at 1,500 RPM and the supernatant frozen at -20°C until treatment of 3D cell cultures.

3D Bovine Endometrial Cell Culture and Treatment

The 3D bovine endometrial cell cultures were established as previously described by MacKintosh et al. [32] with modifications. Briefly, nine days prior to treatment, epithelial cells (90,000 or 300 µL of cell suspension at 3 X 10^5 cells/mL) in cell culture media were plated into transwell inserts (MCHT24H48; Millipore-Sigma) hanging over individual wells, containing 800 µL of cell culture media, within a 24 well plate. The Polyethylene terephthalate (PET) (0.4 µm pore size) transwell insert membranes were pre-coated with diluted growth factor reduced Matrigel (Corning; 30 µL of Matrigel diluted 1:8 in FBS free RPMI) following the manufacturer's recommendation. Transepithelial electrical resistance measurements [TEER (Ωcm^2) = (sample in well insert resistance – blank well insert resistance) X membrane area ($0.33 cm^2$)] were recorded with a Millicell ERS-Voltohmmeter (Millipore-Sigma) to verify that cell polarity was met by day of treatment (TEER > 1500 Ωcm^2) [32]. The day before treatment, fibroblast cells (1 mL; 1 X 10^5 cells/mL) were plated in a separate 24-well plate and allowed to attach for 18 h. The next morning (day of treatment) the fibroblast cells were washed with DPBS (1% ABAM) and 800 µL of RPMI (5% FBS, 1% ABAM) (treatment media) was added to the cells. Similarly, 300 µL of treatment media was also added to the epithelial cells in the transwell inserts. The transwell inserts were then added to wells containing the SF to initiate the 3D cell culture (2 h before treatment). During the UFF experiment (Experiment 1) and 2 h after initiating the 3D cultures, transwell insert treatment media was replaced with 300 µL of 1) new treatment media (Control) or 2) new treatment media containing UFF (1:1). During the IFNT experiment (Experiment 2) and 2 h after initiating the 3D cultures, transwell insert treatment media was replaced with 300 µL of 1) new treatment media (Control) or 2) new treatment media

243 containing recombinant ovine IFNT at 100 ng/mL. In both Experiments 1 and 2, treatments
244 were incubated with the cells for 6 h at 38.8°C in 5% CO_2 and humidified air.
245 In both experiments, 3D cultures were established with uterine-matched epithelial and
246 SF cells from a number of different reproductive tracts. During Experiment 1, a UFF treatment
247 was lost and therefore data represent 5 and 4 uteri for the Control and UFF treatments,
248 respectively (n=4-5). During Experiment 2, a recombinant IFNT treatment was lost and
249 therefore data represent 4 and 3 uteri for the Control and IFNT treatments, respectively (n=3-
250 4). During Experiments 1 and 2 and for each reproductive tract, each treatment was repeated
251 three times; that is, each treatment was applied to three separate 3D cell cultures for each
252 reproductive tract. During sample collection, epithelial cell RNA from the three separate 3D cell
253 cultures (representing a single treatment) were isolated together (RNA was pooled) using an
254 RNA isolation kit (described below). The same was true for the SF below the transwell insert.
255
256 *Epithelial-PET Transwell Membrane Hematoxylin and Eosin Staining*
257 To observe epithelial cells within the transwell inserts, epithelial cells within inserts
258 were fixed, sectioned, and stained with hematoxylin and eosin. Briefly, the cells were fixed by
259 adding 2% neutral buffered formalin in DPBS to the insert and well below (24 well plate) for 20
260 min at R.T. The insert PET membrane was removed using a scalpel and embedded in a block of
261 2% agarose prepared with distilled water. The block was submerged in DPBS before processing
262 and embedding in paraffin wax. Membrane sections (4 µm) on microscope slides were
263 deparaffinized with xylene and rehydrated through a series of diluted ethanol solutions in
264 distilled water before being submerged and held in DPBS. The sections were stained for 5 min

in hematoxylin (Gill No. 2; Sigma), rinsed with tap water for 2 min, submerged in 95% ethanol for 1 min and then stained for 1.5 min in eosin Y (Sigma) before being dehydrated through a series of diluted ethanol solutions in distilled water. The sections were held in 100% ethanol until a coverslip was mounted over the section with glycerol. Images of the epithelial cells and PET transwell membrane were taken under oil emersion using a Nikon Eclipse 80i microscope.

3D Cell Culture Cytotoxicity Assays (MTT Assays)

The 3D cell cultures used during cytotoxicity assays were prepared and treated as described above in Experiment 2 with the addition of a cytotoxic positive control treatment consisting of 0.05% TX-100 in treatment media. Transwell inserts and wells containing medium without cells served as no cell, blank, controls. Briefly, 6 h after treatment, transwell inserts and wells below containing epithelial and SF cells, respectively, were washed with pre-warmed DPBS and new, serum-free, cell culture media containing 3-(4,5-Dimethylthiazol-2-yl)-2,5-diphenyltetrazolium bromide (MTT; Sigma) at a 1:10 dilution (0.5 mg/mL) was added. The 3D cultures were incubated with the MTT for 4 h at 37°C and 5% CO_2 and atmospheric oxygen. At the end of the incubation, the transwell inserts were transferred to a new 24 well plate, cell culture media was removed and 400 µL of 0.04N HCl in isopropanol was added to the transwell inserts and wells containing SF. The 24 well plates were placed in an incubated shaker and shaken at 37°C for 5 min at 150 RPM. Following incubation, a 100 µL sample from each transwell insert and well was transferred to a 96 well plate and the sample absorbance (optical density; OD) read at 570 nm on an Asys Uvm 340 microplate reader (Biochrom). The reference absorbance was set at 630 nm. The OD data were normalized over the blank control.

287

288 *RNA Isolation, RNA-Sequencing (RNA-Seq) and Gene Ontology Analysis*

289 Total RNA was extracted from epithelial (transwell insert) and SF (wells) during
290 Experiment 1 using the E.Z.N.A. Total RNA Kit I (Omega Bio Tek) and during Experiment 2 using
291 the Qiagen RNeasy Kit (Qiagen) according to the manufacturer's recommendations but with
292 modifications. Briefly, for each treatment, media was aspirated from the three transwell inserts
293 and the PET membranes were removed using a sterile scalpel blade. All three membranes were
294 submerged and agitated in 350 µL of lysis buffer supplied by the RNA isolation kit in a 1.5 mL
295 microcentrifuge tube. Medium was then aspirated from wells containing SF and 350 µL of lysis
296 buffer was added to each. Molecular grade ethanol (70%; 350 µL) was then added to the
297 epithelial lysate in the microcentrifuge tube as well as the three SF wells. For each treatment, a
298 single epithelial lysate, representing epithelial cells from three 3D cultures, was applied to a
299 spin column. The three SF lysates were applied to a single spin column by reloading the column
300 after centrifugation of each well lysate until all three wells were complete. The epithelial and SF
301 lysates were centrifuged (microcentrifuge) at 10,000 x g for 1 min and RNA was isolated in
302 accordance with the Omega Bio Tek or Qiagen kit recommendations. The concentration and
303 integrity of epithelial and SF RNA for each treatment was determined using NanoDrop
304 (NanoDrop ND-1000, NanoDrop Technologies) and Bioanalyzer (2100 Bioanalyzer, Agilent
305 Technologies), respectively. The sample RNA integrity numbers (RIN) ranged from 8.6-10.0 and
306 RNA was stored at -80°C.

307 The RNA library preparation and RNA-Seq was conducted by the University of Missouri
308 DNA Core facility as previously described by Moraes et al. [37]. The raw sequences (fastq)

underwent adapter removal and quality trimming utilizing Trimmomatic [38]. The quality reads were then mapped to the bovine reference genome ARS-UCD1.2 using Hisat2 mapper, a sensitive and fast alignment program of next-generation sequencing data [39]. The sorted binary alignment maps and the NCBI gene annotation of the ARS-UCD1.2 assembly were subjected to FeatureCounts [40] to quantify read counts of genes for each sample. Differential gene expression analysis between sample groups was performed by robustly fitting the expression data to a weighted generalized linear model (GLM) using edgeR robust [41].

Gene Ontology (GO) analysis was performed for statistically significant transcripts identified by RNA-Seq using the Database for Annotation, Visualization and Integrated Discovery (DAVID) Bioinformatics Resource 6.8 [42]. Pathway analyses included DAVID enriched biological processes (BP) and the Kyoto Encyclopedia of Genes and Genomes (KEGG). During annotation, the GO Direct category was used which provides mappings directly annotated by the source database. The GO Direct and KEGG categories were considered enriched when $P \leq 0.05$ with the false discovery rate (FDR) ≤ 0.05.

cDNA Synthesis and Quantitative Reverse Transcription PCR (RT-qPCR)

Quantitative reverse transcription PCR was used to validate the data obtained from RNA-Seq and to compare treated cell relative gene expression. Complementary DNA was synthesized using the High Capacity cDNA Reverse Transcription Kit (Applied Biosystems) following the manufacturer's recommendations. Briefly, 500 ng of RNA and nuclease-free water was added to 10 µL of cDNA master mix to reach a total volume of 20 µL. No-reverse transcriptase control samples were also prepared. Following a 2 h cDNA synthesis reaction at

37°C, a cDNA pool was made (5 µL of each sample) and the remaining cDNA was diluted 1:20 using nuclease-free water. Pooled cDNA was used to generate seven standards (1:4 serial dilutions). Standards were used to calculate primer efficiencies (E) using the following equation: $E = [10^{(-1/slope)}-1]$ (Table 1). The slope is the observed RT-qPCR Ct (threshold cycle) values obtained plotted against the Log10 value for each of the seven standard dilutions. Percent efficiency was calculated by dividing E by 2 and multiplying by 100.

The CFX96 Real-Time PCR machine (Bio-Rad Laboratories) was used to perform RT-qPCR reactions. Primer sequences were previously published or designed using Primer3Plus (P3P; Version 2.4.2) (Table 1). Only primers with amplification efficiencies ranging from 90-110 were used. Sample RT-qPCR reactions were carried out in 20 µL reactions in duplicate and consisted of 10 µL of SYBR Green Master Mix (Applied Biosystems), 1.2 µL of forward and reverse primer mix (1 µM final concentration), 2.6 µL nuclease-free water, and 5 µL of cDNA template (6.25 ng RNA equivalent). All experiment samples, including no-reverse transcriptase controls and no-template controls (water in place of cDNA), were assayed in a single 96-well RT-qPCR plate for each target. Thermo-cycling conditions consisted of 50°C for 2 min, 95°C for 2 min, followed by 40 cycles of 95°C for 15 sec and 60°C for 1 min. A disassociation analysis was included for each primer set and the presence of a single, sharp peak was confirmed. The RT-qPCR amplicon lengths were verified using gel electrophoresis (0.8% agarose gel, 1X Tris/Borate/EDTA Buffer, and 0.5 µg/mL ethidium bromide) and a 50 bp DNA ladder (New England BioLabs). Gels were visualized under ultra-violet (UV) light using the DigiDoc-It Imaging System (Analytik Jena).

The qbase+ package (Biogazelle) was used to identify reference genes and calculate relative gene expression values. Briefly, for each experiment, a panel of eight prospective genes

353 [43] were assayed across a subset of cDNA samples to identify two reference genes (geNorm *M*
354 ≤ 0.5; [44, 45]). Experiment 1 target gene expression was normalized to the sample Ct
355 geometric mean of peptidylprolyl isomerase A (*PPIA*) and succinate dehydrogenase complex
356 flavoprotein subunit A (*SDHA*). Experiment 2 target gene expression was normalized to the
357 sample Ct geometric mean of *SDHA* and ring finger protein 11 (*RNF11*). The reference gene
358 geometric means (normalization factor; NF) were used to generate normalized relative
359 quantities (NRQ) for each target using a generalized delta-delta quantification cycle method
360 (ΔΔCq, also known as ΔΔCt) [44]. NRQ values were log10 transformed prior to statistical
361 analysis.
362
363 **Statistical Analysis**
364 The transformed NRQ (Experiment 1 and 2) and normalized MTT OD (Experiment 2) data were
365 analyzed using a general linear model procedure (Proc GLM) in the statistical analysis software
366 (SAS Institute Inc). The procedure tested for an effect of treatment (UFF or IFNT) on relative
367 gene expression and OD (cell viability or cytotoxicity). The epithelial and SF data were analyzed
368 separately. Residual data were scrutinized for normality using the PLOTS=(diagnostics residuals)
369 statement and corrected for normality, when appropriate, using a square root (Sqrt)
370 transformation. Data are presented as non-transformed least squares means ± standard error
371 of the least squares means (LSM ± SEM). A statistically significant difference was declared at P ≤
372 0.05.
373
374 **Results**

Experiment 1: The effect of pregnant ovine UFF on bovine endometrial epithelial and SF gene expression in 3D culture

Prior to testing the effect of recombinant ovine IFNT on bovine endometrial cell gene expression (Experiment 2), 3D cultures were treated with Day 14 pregnant ovine UFF to test endometrial cell responsiveness to conceptus secretory factors including IFNT. Interferon stimulated gene 15 (*ISG15*) and lectin, galactoside-binding, soluble, 3 binding protein (*LGALS3BP*), genes stimulated by IFNT (i.e. ISGs) in bovine endometrium, as well as genes considered to be important for the establishment of pregnancy in mammals, C-X-C chemokine receptor 4 (*CXCR4*) and leukemia inhibitory factor (*LIF*), were measured. Compared to Control epithelial (0.50 ± 5.31) and SF (0.27 ± 11.28), treating 3D bovine endometrial cell cultures with Day 14 pregnant ovine UFF resulted in greater epithelial (130.27 ± 5.94; $P < 0.001$) and SF (58.34 ± 12.61; $P < 0.001$) *ISG15* expression, respectively (Figure 2). The same was true for the expression of *LGALS3BP*. Compared to Control epithelial (0.98 ± 0.23) and SF (0.73 ± 0.30), expression of *LGALS3BP* was greater in epithelial (4.12 ± 0.25; $P < 0.001$) and SF (1.77 ± 0.33; $P < 0.05$), respectively, when 3D cultures were treated with the UFF (Figure 2). Compared to Control epithelial (5.12 ± 1.28) and SF (0.19 ± 0.14), treating 3D bovine endometrial cell cultures with UFF resulted in greater epithelial (9.50 ± 1.43; $P < 0.05$) but not SF (0.41 ± 0.16) *CXCR4* expression, respectively (Figure 2). A similar observation was made for *LIF*. Compared to Control epithelial (4.27 ± 0.86) and SF (0.27 ± 0.09), expression of *LIF* was greater in epithelial (7.11 ± 0.97; $P = 0.05$) but not SF (0.27 ± 0.11), respectively, when treated with UFF (Figure 2).

Experiment 2: The effect of recombinant IFNT on endometrial epithelial and fibroblast cell cytotoxicity

The effect of recombinant ovine IFNT on bovine endometrial epithelial and SF cytotoxicity (viability) during 3D culture was tested. Additional 3D cultures were treated with 0.05% TX-100 as a cytotoxic positive control. Compared to the medium only (Control) treated epithelial (0.63 ± 0.02) and SF (0.10 ± 0.01), only the cytotoxic positive control affected epithelial (0.02 ± 0.02; $P < 0.001$) and SF (0.01 ± 0.01; $P < 0.001$) cell viability. Viability of recombinant IFNT treated epithelial (0.58 ± 0.02) and SF (0.08 ± 0.01) cells was similar to controls.

Experiment 2: Effect of recombinant IFNT on endometrial epithelial and fibroblast cell transcriptomes in 3D culture

There were 8,946 differentially expressed transcripts between control epithelial and SF cells (Supplementary File 1). Of these transcripts, 4,474 and 4,472 were up- and down-regulated, respectively. The top ten most up-regulated transcripts (from most to least) in the SF were 1) fibroblast growth factor 7 (*FGF7*), 2) R-spondin 3 (*RSPO3*), 3) T-box 18 (*TBX18*), 4) sodium voltage-gated channel alpha subunit 3 (*SCN3A*), 5) MAS related GPR family member F (*MRGPRF*), 6) PR/SET domain 12 (*PRDM12*), 7) protocadherin 11-X linked (*PCDH11X*), 8) homeobox D11 (*HOXD11*), 9) heart and neural crest derivatives expressed 2 (*HAND2*), and 10) Wnt family member 2 (*WNT2*) (Supplementary File 1). The top 10 most down-regulated (from most to least) in the fibroblast cells were 1) nephronectin (*NPNT*), 2) UDP glucuronosyltransferase family 1 member A1 (*UGT1A1*), 3) family with sequence similarity 101

418 A (*FAM101A*), 4) fucosyltransferase 6 (*FUT6*), 5) EPH receptor B2 (*EPHB2*), 6) immunoglobulin
419 like domain containing receptor 1 (*ILDR1*), 7) ADAM metallopeptidase with thrombospondin
420 type 1 motif 16 (*ADAMTS16*), 8) prolactin induced protein (*PIP*), 9) claudin 7 (*CLDN7*), and 10)
421 doublecortin domain containing 2 (*DCDC2*). When 3D cell cultures were treated with IFNT, the
422 number of differentially expressed transcripts in the SF compared to the epithelial cells
423 decreased to 7,558 (3385 and 4173 were up- and down-regulated, respectively; Supplementary
424 Figure 1).

425 Compared to control epithelial and SF cells in 3D culture, treatment of 3D cultures with
426 IFNT resulted in 673 and 83 DEGs in the epithelial and SF cells, respectively ($P \leq 0.001$; FDR $P \leq$
427 0.05; Supplementary Figure 2). In an attempt to identify a gene of origin for unidentified
428 transcripts differentially expressed in the epithelial (71) and SF cells (12) in response to IFNT,
429 the unidentified transcript sequences were aligned (BLAST) with sequences published in
430 Ensemble and National Center for Biotechnology Information (NCBI) databases. Some of the
431 uncharacterized sequences corresponded to a single gene (>98% homology), resulting in the
432 identification of 663 (622 up- and 41 down-regulated DEGs) and 80 (all up-regulated) DEGs in
433 the IFNT-treated epithelial and SF cells, respectively (Figure 3). The DEGs were considered IFNT
434 dependent epithelial (Td-Epi) and IFNT dependent SF (Td-SF) DEGs. Almost all (79) Td-SF DEGs
435 were in common with the Td-Epi DEGs (Figure 3). Zinc finger CCCH-type antiviral protein 1
436 (*ZC3HAV1*), also known as zinc-finger antiviral protein (*ZAP*) and poly(ADP-ribose)
437 Polymerase13 (*PARP13*), was uniquely differentially expressed in the SF (up-regulated) when 3D
438 cultures were treated with IFNT (Figure 3).

The 10 most up-regulated (most to least) DEGs in the Td-Epi group were 1) basic leucine zipper ATF-like transcription factor 2 (*BATF2*), 2) MX dynamin like GTPase 2 (*MX2*), 3) interferon induced protein 44 (*IFI44*), 4) interferon-induced protein with tetratricopeptide repeats 1 (*IFIT1*), 5) 2'-5'-oligoadenylate synthase 2 (*OAS2*), 6) cyclic nucleotide gated channel beta 1 (*CNGB1*), 7) placenta-specific 8 (*PLAC8*), 8) kinesin family member 5C (*KIF5C*), 9) serum amyloid A4 constitutive (*SAA4*), and 10) Z-DNA binding protein 1 (*ZBP1*) (Figure 3).

The 10 most down-regulated (least to most) DEGs in the Td-Epi group were 1) microtubule associated protein 6 (*MAP6*), 2) histone H3.1 (*HIST1H3A*), 3) zinc finger MYND-type containing 10 (*ZMYND10*), 4) protocadherin alpha-5 (*PCDH45*), 5) GVQW motif containing 3 (*GVQW3*), 6) family with sequence similarity 92 member A (*FAM92A*), 7) secernin 1 (*SCRN1*), 8) Kruppel like factor 13 (*KLF13*), 9) solute carrier family 25 member 15 (*SLC25A15*), and 10) fat storage inducing transmembrane protein 2 (*FITM2*) (Figure 3).

The 10 most up-regulated (most to least) DEGs in the Td-SF were 1) *OAS2*, 2) interferon induced protein 44 like (*IFI44L*), 3) radical S-adenosyl methionine domain containing 2 (*RSAD2)*, 4) *ZBP1*, 5) 2'-5'-oligoadenylate synthase 1Y (*OAS1Y*), 6) *MX2*, 7) *MX1,* 8) *PLAC8,* 9) *IFI44* and 10) TNF superfamily member 10 (*TNFSF10*) (Figure 3).

Experiment 2: Conceptus-induced, IFNT-dependent endometrial DEGs detected in endometrial epithelial and fibroblast cells treated with IFNT during 3D culture.

In an effort to focus on more physiologically relevant ISG, the 663 Td-Epi and 80 Td-SF DEGs were then compared to a list of 369 conceptus-induced IFNT-dependent endometrial DEGs (CiTd-Endo) genes previously identified as differentially expressed in intact, mid-luteal

phase, bovine endometrium treated with recombinant ovine IFNT or Day 15 bovine conceptuses [30](Figure 4). Overall, the endometrial epithelial and/or SF cells treated with IFNT during 3D culture shared 224 DEGs (all up-regulated) in common with the CiTd-Endo DEGs (Figure 4; Regions I, II, and III; broken circle). Sixty-nine DEGs were shared between all three groups (CiTd-Endo, Td-Epi, and Td-SF; Figure 4; Region II). One hundred and fifty-four DEGs were shared exclusively between the CiTd-Endo and Td-Epi groups (Figure 4; Region I). Only 1 DEG (*ZC3HAV1*) was shared exclusively between CiTd-Endo and Td-SF groups (Figure 4; Region III) indicating that endometrial expression of this gene in response to conceptus IFNT is SF specific. A complete list of DEGs found in common or uncommon between groups (Regions I-VI) within the Venn diagram (Figure 4) can be found in Table 2.

The DEG LogFC values in this study and in Mathew et al. [30] varied across endometrial cell types treated with IFNT during 3D culture (epithelial and SF cells) and endometrium treated with IFNT or Day 15 bovine conceptuses (Supplementary File 3). Interestingly, however, the 69 DEG (Figure 4, Region II) average LogFC values for endometrium treated with Day 15 bovine conceptuses and IFNT as well as bovine endometrial epithelial and SF cells treated with IFNT during 3D culture were similar (4.17, 4.32, 4.65, and 4.14, respectively; 69 DEG LogFC average; Supplementary File 3). These values were greater than the 154 DEG (Figure 4; Region I) average LogFC values for endometrium treated with Day 15 bovine conceptuses and IFNT and endometrial epithelial cells treated with IFNT during 3D culture (1.74, 1.84 and 1.90, respectively, 154 DEG LogFC average; Supplementary File 3). When DEG LogFC values were averaged across studies for each of the 224 common DEGs, all of the top 10 most highly expressed DEGs were those found in common between CiTd-Endo, Td-Epi, Td-SF groups (Figure

4; Region II) (Supplementary File 3). From greatest to least expressed these DEGs were 1) *MX2*, 2) *IFI44*, 3) *IFIT1*, 4) *RSAD2*, 5) interferon-induced protein with tetratricopeptide repeats 1 (*IFIT3*), 6) *OAS2*, 7) *ISG15*, 8) *BATF2*, 9) *IFI44L*, and 10) *ZBP1*. Of the 224 common DEGs, epithelial cell expression of *BATF2* (LogFC 11.88) followed by epithelial *MX2* (LogFC 10.26) and *IFI44* (Log FC 9.95) was greatest in this study (Supplementary File 3).

The top 10 most highly expressed DEGs shared between CiTd-Endo and Td-Epi groups but were not detected in SF (Figure 4; Group I) were, from greatest to least expressed, 1) guanylate-binding protein 2 (*GBP2*), 2) indoleamine 2,3-dioxygenase 1 (*IDO1*), 3) *KIF5C*, 4) *GBP6*, 5) forkhead box S1 (*FOXS1*), 6) TNF superfamily member 13B (*TNFSF13B*), 7) atypical chemokine receptor 4 (*ACKR4*), 8) G protein subunit gamma transducin 2 (*GNGT2*), 9) growth hormone secretagogue receptor (*GHSR*), and 10) schlafen family member 11 (*SLFN11*) (Supplementary File 3).

Experiment 2: Gene Ontology (GO) analysis of conceptus-induced, IFNT-dependent endometrial DEGs detected in endometrial epithelial and fibroblast cells treated with IFNT during 3D culture.

The GO analysis of the 223 DEGs shared between the CiTd-Endo and Td-Epi groups (Figure 4; Regions I and II) identified 16 enriched BP ($P \leq 0.001$; FDR $P \leq 0.05$; Table 3; Supplementary File 4). The top five enriched processes (from greatest to least) include 1) type I interferon signaling pathway, 2) defense response to virus, 3) interferon-gamma mediated signaling pathway, 4) response to virus, and 5) negative regulation of viral genome replication. The KEGG pathway analysis identified 5 enriched pathways including, from greatest to least, 1)

505 influenza A, 2) herpes simplex infection, 3) hepatitis C, 4) measles, and 5) RIG-1-like receptor
506 signaling pathway (P ≤ 0.001; FDR P ≤ 0.05; Table 3; Supplementary File 4).
507 The GO analysis of the 70 DEGs shared between CiTd-Endo and Td-SF groups identified
508 12 enriched BP (P ≤ 0.001; FDR P ≤ 0.05; Table 3). The top five enriched processes (from
509 greatest to least) include 1) defense response to virus, 2) type I interferon signaling, 3) response
510 to virus, 4) negative regulation of viral genome replication, and 5) interferon-gamma-mediated
511 signaling pathway. The KEGG pathway analysis identified five enriched pathways including,
512 from greatest to least, 1) influenza A, 2) herpes simplex infection, 3) measles, 4) RIG-I-like
513 receptor signaling, and 5) hepatitis C (P ≤ 0.001; FDR P ≤ 0.05; Table 3). A list of BP and KEGG
514 pathways based on the FDR, Bonferroni correction, and Benjamini-Hochberg procedure can be
515 found in Supplementary File 4.
516
517 *Experiment 2: Conceptus induced, IFNT dependent endometrial DEGs not detected in*
518 *endometrial epithelial and stroma fibroblast cells treated with IFNT during 3D culture.*
519
520 There were 145 CiTd-Endo DEGs (Figure 4, Region V), of which 132 and 13 were up- and
521 down-regulated, respectively, that were not differentially expressed in the endometrial
522 epithelial or SF when 3D cultures were treated with IFNT. Of these, the top 10 most highly
523 expressed endometrial DEGs within the IFNT treated explants [30] but missing in the epithelial
524 or SF, from greatest to least, were 1) C-type lectin domain family member 4 F (*CLEC4F*), C-C
525 motif chemokine ligand 8 (*CCL8*), C-X-C motif chemokine ligand 11 (*CXCL11*), (*CXCL10*), T cell
526 immunoglobulin and mucin domain containing 4 (*TIMD4*), apolipoprotein B mRNA editing

enzyme, catalytic peptide-like 3A (*APOBEC3Z1*), *OAS1*, guanylate binding protein 7 (*GBP7*), proteasome 20S subunit alpha 8 (*PSMA8*), and the GTPase, very large interferon inducible pseudogene (*GVINP1*) (Supplementary File 5). The 13 missing down-regulated DEGs (Figure 4, Region V), from greatest to least down-regulated, were: 1) jagged canonical notch ligand 1 (*JAG1*), LIM domain binding 2 (*LDB2*), KIT proto-oncogene receptor tyrosine kinase (*KIT*), carbohydrate sulfotransferase 15 (*CHST15*), family with sequence similarity 101, member B (*FAM101B* or *Refilin B*), platelet and endothelial cell adhesion molecule 1 (*PECAM1*), cluster of differentiation 93 (*CD93*), actin filament associated protein 1 like 1 (*AFAP1L1*), family with sequence similarity 124 member B (*FAM124B*), apelin receptor (*APLNR*), SRY-Box transcription factor 18 (*SOX18*), phosphatase domain containing paladin 1 (*PALD1*), and vasohibin 1 (*VASH1*) (Supplementary File 5).

The GO analysis identified Inflammatory response; ($P \leq 0.001$; FDR $P \leq 0.05$) as the only BP associated with the 133 DEGs found to be up-regulated in explants treated with Day 15 conceptuses and IFNT (CiTd-Endo) but missing in endometrial epithelial or SF cells (Supplementary File 5). The 15 factors associated with the Inflammatory response pathway were: 1) Complement C3A receptor 1 (*C3AR1*), complement C4A (*C4A*), gasdermin D (*GSDMD*), *CXCL9*, *CCL8*, toll-like receptor 4 (*TLR4*), interleukin 15 (*IL15*), *CD40*, *CXCL11*, extracellular matrix protein 1 (*ECM1*), *CXCL10*, *IL23A*, receptor interacting serine/threonine kinase 2 (*RIPK2*), and FAS cell surface death receptor (*FAS*). The 13 down-regulated DEGs were not associated with a BP. Further, no KEGG pathways were identified for the up- or down-regulated CiTd-Endo DEGs not detected in the endometrial epithelial or SF cells treated with IFNT during 3D culture.

549 *Experiment 2: RNA-Seq and RT-qPCR Data Validation*

550 The RT-qPCR was utilized to validate the RNA-Seq results. Overall, the expression of 12
551 genes in the Control and IFNT treated epithelial and SF cells from 3D cultures were assayed.
552 These genes included *MAP6* (Figure 4, Region VI; down-regulated in epithelial cells), signal
553 transducer and activator of transcription 1 (*STAT1)*, *IDO1*, *LGALS3BP*, and tumor necrosis factor
554 super family member 13 B (*TNFSF13B*) (Figure 4, Region I; up-regulated in epithelial cells), *MX1*,
555 *MX2*, *ISG15*, lectin, galactoside-binding, soluble, 9 (*LGALS9*), *OAS2*, *BATF2* (Figure 4, Region II;
556 up-regulated in epithelial and fibroblast cells), and *ZC3HAV1* (Figure 4, Region III; up-regulated
557 in the fibroblast cells) (Table 4 and Figure 5). Overall, the epithelial and SF cell relative
558 expression status (up- or down-regulated; LogFC) compared to Controls for all genes assayed by
559 RT-qPCR were consistent with the RNA-Seq data. Compared to the Control epithelial cells, a
560 statically significant effect of IFNT on epithelial expression of *STAT1*, *IDO1*, or *MAP6* was not
561 detected by RT-qPCR, however, their relative status of expression (up or down-regulated)
562 compared to Controls aligned with the RNA-Seq results. Conversely, statistical analysis of the
563 RT-qPCR data but not the RNA-Seq data, identified *LGALS3BP* and *TNFSF13B* as DEGs also up-
564 regulated in SF cells treated with IFNT during 3D culture (Table 4 and Figure 5).

565

566 **Discussion**

567 The aim of this study was to investigate the effects of IFNT, a type I interferon secreted
568 by the early bovine conceptus and MRP signal, on bovine endometrial epithelial and SF cell
569 transcriptomes in a 3D co-culture environment. Major findings of the study include: 1)
570 identification of IFNT-stimulated genes in bovine endometrial epithelium and SF cells, 2)

identification of bovine endometrial cell types responsible for conceptus-induced, IFNT-dependent endometrial DEGs and 3) identification of conceptus-induced, IFNT-dependent BP in bovine endometrial epithelial and SF cells.

Recent studies have utilized 3D bovine endometrial cell cultures involving co-culture of endometrial epithelial over SF cells on a semipermeable membrane to model uterine innate immune responses to bacterial lipopolysaccharides and lipopeptides [32, 33]. In this study, we employed a 3D bovine endometrial cell culture system to model the effects of IFNT, the ruminant MRP signal, on endometrial epithelial and SF cell transcriptomes. The 3D endometrial cell cultures have the advantage of mimicking the endometrial surface architecture while allowing for important paracrine communication between the uterine epithelia and SF. Further, the polarized epithelial and underlying SF mRNAs, proteins, or secretions may be collected to gain important information regarding endometrial cell-specific responses to conceptus secretory factors such as IFNT; this cell specificity cannot be achieved with endometrial explants or uterine biopsies. Using a similar bovine endometrial cell isolation and culture technique as described here, Herath et al. [46] reported epithelial and SF cell culture purities greater than 95% with undetectable levels of CD45 (common leukocyte antigen) mRNA and protein. Li et al. [35] also reported that primary bovine endometrial epithelial cells did not exhibit significant changes in morphology or cell marker gene expression alterations after 20 passages. Similarly, we did not notice changes in the epithelial or SF cell morphology after multiple passages or days in culture. Upon attachment, epithelial and SF cell morphologies were clearly different, allowing us to visually assess the two populations over time (Figure 1). Further, ICC for

cytokeratin, an epithelial cell marker, in the epithelial and SF cultures indicated nearly complete separation of the two cell types prior to 3D culture (Figure 1).

Bovine Endometrial Epithelial and SF Transcriptomes

Compared to the Control epithelial cells from 3D cultures, RNA-Seq identified 8,946 transcripts that were differentially expressed in the Control SF cells. The most differentially expressed transcript in the SF compared to the epithelium was *FGF7* which was approximately 26,000-fold greater (LogFC 14.67). Typically expressed in tissues of mesenchyme origin, FGF7 stimulates epithelial cell proliferation via its receptor, fibroblast growth factor receptor 2b (FGFR2b) [47]. In sheep and primates, *FGF7* is expressed within the endometrial stroma [48, 49]. Bovine endometrial cells also express *FGF7* and although its mRNA and protein have not been localized within the tissue, it is believed to be expressed within the endometrial stroma [50]. In cattle, both the endometrium and conceptus tissues express FGFR2b [50, 51]. FGF7 has been shown to stimulate pig trophectoderm proliferation and Cooke et al. [50] reported that recombinant human FGF7 stimulated *IFNT* expression in bovine trophectoderm cells in a dose-dependent manner [52]. Importantly, FGF7 is highly expressed within isolated bovine endometrial SF and may partially explain why endometrial fibroblast cell conditioned media stimulates bovine trophectoderm proliferation and outgrowth in culture [51].

Conceptus-Induced, IFNT-Dependent Endometrial (CiTd-Endo) DEGs

Sixty-one percent (224 of 369) of the CiTd-Endo DEGs identified by Mathew et al. [30] overlapped with the Td-Epi and/or Td-SF DEGs (Figure 4). The status of expression for all the

614 overlapping DEGs was the same between the two studies. That is, all 224 common DEGs were
615 up-regulated in this study and that of Mathew et al. [30]. Of these 224 DEGs, 154 were within
616 the Td-Epi group alone, 69 were shared between the Td-Epi and Td-SF groups and one DEG
617 (*ZC3HAV1*) was within the Td-SF group alone (Figure 4). Epithelial and/or SF LogFC values for
618 the 224 DEGs varied between cell type (this study) and intact endometrium treated with Day 15
619 bovine conceptuses or IFNT [30], however, they were similar (Supplementary File 3).
620 Approximately 39% (145 of 369) of the CiTd-Endo DEGs identified by Mathew and
621 others [30] were not differentially expressed in the endometrial epithelial or SF cells treated
622 with IFNT (Supplementary File 5). Those not differentially expressed included chemokine
623 molecules *CCL8*, *CXCL9*, *CXCL10*, and *CXCL11* that are commonly expressed in leukocytes and
624 up-regulated within the endometrium during early pregnancy in cattle [30, 53-55]. Also
625 included within this list was solute carrier (SLC) transporter *SLC2A6* (also known as GLUT6 or
626 GLUT9), a glucose transporter expressed in lymphocytes and macrophages [56]. Indeed, GO
627 analysis identified inflammatory response as a major BP associated with the missing DEGs. Their
628 expression within bovine endometrial leukocytes would explain why they were detected in
629 intact endometrium treated with conceptuses or IFNT [30] but not in IFNT treated epithelial or
630 SF cultures.
631
632 *Type I IFN Signaling*
633 Type I IFNs are secreted by cells during viral infection and TLR activation by viral RNAs
634 [19, 57]. In turn, type I IFNs activate the janus associated kinase-signal transducer and activator
635 of transcription (Jak-STAT) signaling pathway and up-regulate ISGs, interfering with viral

636 replication and enhancing recognition of infection through up-regulation of MHC class I
637 molecules [58]. Type I IFN signaling involves activation of STAT1 and STAT2 transcription factors
638 which dimerize and associate with, interferon regulatory factor 9 (IRF9), forming the interferon-
639 stimulated gene factor 3 (ISGF3) transcription factor complex [19, 57]. The ISGF3 complex binds
640 IFN-stimulated response elements (ISRE) within gene promoter regions, up-regulating what are
641 considered classical ISGs that interfere with viral replication [19, 22, 57]. Other interferon
642 regulatory factor (IRF) family members in addition to IRF9 may be expressed or activated during
643 type I IFN signaling. The IRFs bind interferon regulatory factor elements (IRFEs) or ISREs and
644 depending on the IRF, target gene expression may be activated or repressed. IRF1, IRF3, IRF5,
645 IRF7, and IRF9 are typically considered activators and while IRF2 and IRF8 are described as
646 repressors. Some IRFs, including IRF2, IRF4, IRF5, IRF7, and IRF8 have both activator and
647 repressor activities [59]. Type I IFN signaling can also activate the mitogen activated protein
648 kinases (MAPK) and phosphatidyl inositol 3 kinase (PI3K) signaling pathways [19, 22, 23].
649 Importantly, when an IRF repressor is active, classical ISG expression may be reduced and type I
650 IFN activation of second messenger pathways independent of STAT such as of PI3K, MAPK, and
651 subsequently, activation of NFKB transcription factors, can induce expression of what are
652 considered non-classical ISGs [20, 25, 57].
653
654 *IFNT and Maternal Recognition of Pregnancy*
655 IFNT is a type I IFN secreted by the ruminant conceptus that serves as the MRP signal by
656 disrupting the endometrial luteolytic mechanism to maintain ovarian P4 secretion and
657 subsequently, pregnancy [7]. To achieve this, conceptus IFNT induces endometrial ISG

658 expression and disrupts uterine epithelial pulse secretion of $PGF_{2\alpha}$. Thus, IFNT "rescues" the CL
659 from luteolysis via an anti-luteolytic mechanism to maintain ovarian P4 secretion [7]. In sheep
660 and cattle, IFNT stimulated endometrial IRFs are hypothesized to have essential functions
661 related to the anti-luteolytic mechanism and ISG expression. Although less information is
662 available for cattle, a working sheep model described by Spencer and others [8] suggests that
663 IFNT stimulates activation of IRF2 within the uterine surface epithelium, silencing expression of
664 *ESR1* and subsequently, *OXTR* expression. Ultimately, this disrupts the pulsatile secretion of
665 $PGF_{2\alpha}$ and luteolysis [23]. IRF2 is exclusively expressed within the uterine luminal and surface
666 glandular epithelium (LE/sGE) where it increases during early pregnancy in sheep [21].
667 Importantly, the *ESR1* but not the *OXTR* promoter region contains two IRFEs and an ISRE for
668 which IRF2 is hypothesized to repress *ESR1* transcription [60]. The *IRF1* promoter also contains
669 an ISRE for which IRF2 is hypothesized to bind and repress IRF1 activity, further reducing
670 expression of classical ISGs in the uterine LE/sGE. Thus, IFNT induced activation of signaling
671 pathways independent of STAT results in expression of non-classical ISGs in the uterine surface
672 epithelium of sheep such as insulin-like growth factor binding protein 1 (*IGFBP1*), Wnt family
673 member 7A (*WNT7A*), and *LGALS15*; the latter a gene not present in cattle [16]. In the ovine
674 uterine SF and deep glandular epithelium (SF/dGE), where IRF2 is absent, IFNT can stimulate
675 IRF1 activity and expression of classical ISGs such as *ISG15*, *MX2*, *OAS2,* and ISGF3 assembly
676 factors [16].
677 Although less information is available for cattle than for sheep, it is generally accepted
678 that IFNT induces classical and non-classical ISG expression within the uterine SF and LE/sGE via
679 activation of IRF1 and IRF2, respectively [16, 24]. Further, during MRP in cattle and unlike

680 sheep, IFNT reduces uterine LE/sGE expression of *OXTR* but not *ESR1* [23, 61]. It has not been
681 determined if IRF2 is involved in the anti-luteolytic mechanism in cattle. However, the bovine
682 *OXTR* promoter contains an ISRE for which both murine IRF1 and IRF2 and similar bovine
683 endometrial cell nuclear extract proteins can bind [62].
684
685 *IFNT Dependent Epithelial and Stroma Fibroblast DEGs*
686 Differentially expressed genes in common with both Td-Epi and Td-SF groups (Figure 4;
687 Region II) included well-known pregnancy or IFNT-stimulated endometrial classical ISGs such as
688 *ISG15*, *MX2*, *OAS2*, and ISGF3 assembly factor, *IRF9* [63]. Although bovine endometrial
689 epithelial cells in the 3D cell culture system establish tight junction proteins and cell polarity,
690 IFNT likely traversed the epithelium to reach the endometrial SF [32, 64]. During early
691 pregnancy in sheep, conceptus IFNT has been shown to traverse the uterine epithelial barrier,
692 reaching circulation and stimulating ISG expression in peripheral blood leukocytes (PBL), liver,
693 and CL [64]. When DEG LogFC values were averaged across tissues from both studies
694 (endometrium and endometrial cells), *MX2* was the most highly expressed gene in response to
695 IFNT or bovine conceptuses (Supplementary File 3). A member of the dynamin-like large GTPase
696 family, MX2 interacts with viral capsule proteins and cDNA, in this way inhibiting viral activity
697 and integration into the host genome [65]. During early pregnancy in cattle, conceptus IFNT
698 induces *MX2* expression in circulating PBL and may be used to diagnose pregnancy [64, 66]. The
699 bovine *MX2* promoter region contains multiple ISREs which would explain why *MX2* is highly
700 expressed in bovine tissues in response to type I IFNs [67].

Many of the DEGs shared between the epithelial and SF cells (Figure 4; Region II) treated with IFNT are considered classical ISGs. In sheep, IFNT stimulated classical ISG expression is largely restricted to the SF/dGE; presumably because of increased activity of IRF2 and inhibition of classical ISG expression in the uterine surface epithelium. It is possible that expression of some IFNT stimulated classical ISGs differ between cattle and sheep. For instance, during early pregnancy in sheep, expression of classic ISG interferon-induced transmembrane protein 3 (IFITM3) appears to be restricted to the stroma stratum compactum; however, *IFITM3* is specifically expressed within the endometrial LE/sGE during early pregnancy in cattle [68, 69]. Genetic differences between cattle and sheep in terms of ISRE and/or IRFE binding sites may partially explain these differences such as in the case of the *ESR1* promoter. Further, the effect of cell isolation and *in vitro* culture on endometrial cell gene expression cannot be excluded. Although endometrial cells were collected during the mid-luteal phase of the estrous cycle and when the conceptus would secrete IFNT, *in vitro* culture for up to two weeks in the absence of reproductive hormones such as P4 could affect endometrial cell ISG expression.

IFNT-Dependent Epithelial and Stroma Fibroblast Interferon Regulatory Factors (IRFs)

Expression of a number of IRF molecules found to be CiTd-Endo DEGs were stimulated by IFNT in the SF and/or epithelial cells during 3D culture. *IRF4*, *IRF7,* and *IRF9* were shared between the epithelial and SF (Figure 4; Region II) while *IRF1*, *IRF2*, *IRF3*, and *IRF8* were detected within the epithelium alone (Figure 4; Region I). Expression of *IRF2* within the epithelium but not SF is consistent with studies of the anti-luteolytic mechanism in ruminants. Although IFNT is hypothesized to stimulate *IRF2* while blocking *ESR1* expression in sheep and

723 *OXTR* expression in cattle, an increase in endometrial epithelial *IRF2* transcription or protein
724 activity in response to IFNT has not been detected[21, 70, 71]. In sheep, *IRF2* expression and
725 protein increases within the endometrium between days 11 and 15 of pregnancy, however, an
726 increase in endometrial *IRF2* was not detected after 5 days of intrauterine infusion of IFNT [21].
727 Further, an IFNT stimulated increase in cytoplasmic or nuclear IRF2 protein could not be
728 detected in immortalized bovine or ovine endometrial epithelial cells, respectively [70, 71]. To
729 the best of our knowledge, this may be the first study to detect an increase in ruminant
730 endometrial epithelial expression *IRF2* in response to IFNT. Expression of *IRF2* was modest in
731 the epithelium and comparable to expression of *IRF1* after 6 h of treatment.
732 A major BP associated with IFNT-induced DEGs in the epithelial cells was positive
733 regulation of the NFKB signaling pathway. Conceptus induced activation of NFKB transcription
734 factors within the uterine LE likely contributes to histotroph synthesis, trophectoderm
735 adhesion, and uterine surface architectural changes during implantation in mammals [28, 72].
736 Transcriptional regulation with the endometrial epithelium in response to IFNT may involve
737 physical interactions between ISGF3, IRF family members, and NFKB. It has been shown that
738 NFKB and ISGF3 or IRF family members, particularly IRF3 and IRF7, directly interact to co-
739 regulate gene expression [28, 73]. These interactions could occur within the bovine *IRF2*
740 promoter which was predicted to have as many as 8 IRF family members and 21 NFKB
741 transcription factor binding sites [74]. These interactions could also involve BATF2. A member
742 of the AP-1 basic leucine zipper transcription factor family, *BATF2* was the most highly
743 expressed transcript detected within the endometrial epithelial cells in response to IFNT that
744 was also identified as a CiTd-Endo DEG (Figure 4; Region II). Typically involved in immune cell

differentiation, BATF2 can interact with IRF1 and the p65 subunit of NFKB to modulate gene transcription [75-77]. Although expression has been detected within epithelial cells, little information is available regarding its function within the mucosa [77]. It was recently reported, however, that IFNG reduced invasive characteristics of an immortalized human trophoblast cell line via the up-regulation of BATF2 [78].

IFNT Dependent Epithelial and Stroma Fibroblast SLC Transporters

Solute carrier (SLC) transporters are a group of cell membrane proteins encoded by over 300 genes that transport micro- and macromolecules [79]. Their expression within the endometrium aids in uterine histotroph production to support developmental processes in the conceptus [80-82]. Four SLC transporters were identified as CiTd-Endo DEGs that were also up-regulated within the endometrial epithelial and SF cells treated with IFNT. An endosomal and lysosomal peptide and histidine transporter, *SLC15A3* (also known as PHT2), was up-regulated in both the endometrial epithelial and SF cells. In line with these findings, Groebner et al. [83] detected an IFNT induced increase in *SLC15A3* expression within co-cultured bovine endometrial glands and SF cells. Expression of *SLC15A3* is greater in pregnant compared to cyclic bovine endometrium on Day 18, concomitant with increased conceptus IFNT secretion [68]. In cattle, intrauterine concentrations of histidine increase during early pregnancy, and histidine is suspected to influence conceptus development [83-85].

Mitochondrial transporters for thiamine pyrophosphate (TPP) (*SLC25A19; also known as DNC)*, iron (*SLC25A28)*, and inorganic anions/malate (*SLC25A30*) were also considered CiTd-Endo DEGs and up-regulated in endometrial epithelial cells by IFNT [30, 86]. SLC25A19

767 transports cytosolic TPP into the mitochondria where it acts as a cofactor for enzymes involved
768 in the tricarboxylic acid (TCA). Little information is available regarding type I IFN regulation of
769 *SLC25A19* and its activity within reproductive tissues. Compared to *in vivo* produced mouse
770 embryos, *in vitro* produced embryos have lower expression of *SLC25A19* [87]. Further, knockout
771 of *SLC25A19* in mice results in erythropoietic failure, reduced central nervous system
772 development, and is embryonic lethal by Day 12 [88]. It was recently discovered that individuals
773 with non-syndromic bilateral striatal necrosis (BSN), a form of a neurological condition
774 frequently associated with mutations within the *SLC25A19* gene and mitochondrial pathologies,
775 can have increased type I IFN signaling [89, 90]. Taken together, data suggest that *SLC25A19* is
776 an ISG, however, its function during early pregnancy in cattle is not known.
777 There is limited information regarding the functions of SLC25A28 and SLC25A30 within
778 reproductive tissues. SLC25A28, also known as Mitoferrin-2, has been identified as a
779 ubiquitously expressed mitochondrial iron transporter [91]. Until recently, the transport
780 properties of SLC25A30 within the mitochondria were not known. A study by Gorgoglione et al.
781 [92]suggests that SLC25A30 may function to export sulfite and thiosulfate to modulate
782 appropriate levels of mitochondrial hydrogen sulfide. In addition, SLC25A30 was able to
783 transport malate which would contribute to the mitochondrial malate-aspartate shuttle and
784 transport of electrons to the inner mitochondrial matrix for oxidative phosphorylation. It may
785 be important to note that malate and malate dehydrogenase are present within the
786 intrauterine environment in cattle and malate has been shown to influence early embryonic
787 development in the hamster [85, 93]. A comprehensive study investigating ISG anti-retroviral
788 activity suggests that SLC25A28 and SLC25A30 may inhibit viral replication [94].

IFNT Dependent Epithelial Growth Hormone Secretagogue Receptor (GHSR)

The growth hormone secretagogue receptor (*GHSR*), also known as the ghrelin receptor, was identified as a CiTd-Endo DEG and was a top 10 most up-regulated gene in the endometrial epithelial cells in response to IFNT. Ghrelin signals through the GHSR to control a number of biological processes related to pituitary growth hormone secretion and growth, food intake, glucose and lipid metabolism, gastrointestinal motility, and secretion and regulation of immune function [95]. Ghrelin and GHSR are present within the reproductive tissues of primates, rodents, and cattle and ghrelin deficiency in mice leads to reduced embryo implantation [96, 97]. In humans, GHSR is expressed by uterine LE cells and reduced expression is associated with poor fertility [98]. Deaver and others [99] detected ghrelin and GHSR within bovine endometrium on Day 7 of the estrous cycle in Holstein heifers. Immunofluorescent staining for ghrelin protein was localized to uterine glands. Staining for the GHSR was less intense compared to ghrelin and described as being within the uterine stroma, however, images of IHC also suggest staining within the endometrial epithelium [99]. It has been shown that supplementing ghrelin to *in vitro* produced rodent and cow embryo culture medium has positive and negative effects on embryonic development depending on concentration [100]. Therefore, an appropriate balance of ghrelin signaling may be critical for the establishment of pregnancy in cattle and other species [99, 100].

IFNT Dependent Stroma Fibroblast ZC3HAV1

One gene, *ZC3HAV1,* which was recently identified as a CiTd-Endo DEG was up-regulated in the endometrial SF cells but not in the epithelium in response to IFNT during 3D culture. Also known as ZAP or PARP13, ZC3HAV1 is an anti-viral protein stimulated by type I IFNs that can bind retroviral RNA leading to its destabilization and reduced translation [101-103]. There is little information regarding *ZC3HAV1* expression or function within reproductive tissues. In human endometrium, LE expression of *ZC3HAV1* decreases between Days 2 and 7 after ovulation coinciding with the time of uterine receptivity [104]. In the Day 8 *in vitro* produced bovine blastocyst, *ZC3HAV1* expression was less within the trophectoderm compared to the inner cell mass (ICM) [105]. Methylation of the *ZC3HAV1* promoter has been shown to restrict *ZC3HAV1* transcription and could explain its tissue-specific expression [106].

In mammals, endogenous retroviral RNAs and proteins are present within the endometrial epithelium and trophectoderm and have important functions during establishment of pregnancy including cell proliferation, immunosuppression, and cell-cell fusion or syncytia formation [107-110]. In sheep, expression of endogenous jaagsiekte retrovirus (*enJSRV*) and *syncytin-Rum1* retroviral RNAs occur within the trophectoderm and uterine epithelium [107, 111, 112]. In addition, endometrial exosomes containing *enJSRV* RNA stimulate sheep trophectoderm IFNT expression possibly through activation of conceptus toll-like receptors (TLR) [113]. Impressively, sheep enJSRV that are shed from the endometrial epithelium can form infectious viral particles that have the capacity to infect bovine blastocysts [111]. Similar to sheep, bovine trophectoderm and endometrial epithelium express bovine endogenous retrovirus (*BERVs*) and *syncytin-Rum1* during early pregnancy [109, 114, 115]. The *BERVs* and *syncytin-Rum1* are expressed within bovine conceptus binucleate cells (BNC) and have

fusogenic activity, likely contributing to the formation of fetal-maternal trinucleate cells (TNC) in formation of the synepitheliochorial placenta [109, 110, 114].

Importantly, it is not understood how ovine or bovine retroviral particles are produced within the trophectoderm and endometrial epithelium in the presence of IFNT, an abundantly secreted type I IFN that induces a number of anti-retroviral genes and processes within these tissues. Considering that *ZC3HAV1*, a repressor of retroviral RNA stability, is in lesser abundance within the trophectoderm compared to the ICM and, compared to bovine endometrial SF cells, was not induced in the endometrial epithelial cells when treated with IFNT, it is possible that reduced expression of *ZC3HAV1* within trophectoderm and endometrial epithelium is somewhat permissive of retroviral gene translation in the presence of IFNT. On the other hand, expression of *ZC3HAV1* within the ICM and uterine stroma may reduce maternal to fetal viral transmission and/or restrict retroviral components to the uterine-placental interface.

Conclusion

This study has identified conceptus-induced, IFNT-dependent DEGs specifically within bovine endometrial epithelial and SF cells. The data provides important information regarding endometrial cell type specific responses to IFNT, a major conceptus secretory factor and the MRP signal in ruminants. A number of well-known and novel ISGs were expressed within both the epithelia and SF cells in response to IFNT. Importantly, 154 DEGs were detected within the epithelial cells alone while 1 DEG, *ZC3HAV1*, was specifically expressed within the SF despite applying IFNT apically to the 3D cultures. Data would suggest that NFKB transcription factors and several IRF molecules in addition to *IRF2* are expressed in the epithelium in response to

IFNT. Interactions between these transcription factors likely control essential processes within the uterine surface epithelium during MRP and implantation. Many of the DEGs described in this study have not been characterized in terms of function and further studies are needed to identify their activities during early pregnancy in cattle. Importantly, inadequate conceptus IFNT secretion during MRP is believed to contribute to early embryonic mortality and a better understanding of IFNT signaling within the endometrium may lead to technologies that mitigate this loss.

References

1. Franco G, Reese S, Poole R, Rhinehart J, Thompson K, Cooke R, Pohler K. Sire contribution to pregnancy loss in different periods of embryonic and fetal development of beef cows. Theriogenology 2020; 154:84-91.
2. Ledoux D, Ponsart C, Grimard B, Gatien J, Deloche MC, Fritz S, Lefebvre R, Humblot P. Sire effect on early and late embryonic death in French Holstein cattle. Animal 2015; 9:766-774.
3. Santos JE, Thatcher WW, Chebel RC, Cerri RL, Galvão KN. The effect of embryonic death rates in cattle on the efficacy of estrus synchronization programs. Anim Reprod Sci 2004; 82-83:513-535.
4. Geary T. Management Strategies to Reduce Embryonic Loss. In. Range Beef Cow Symposium; 2005: 36.
5. Wiltbank MC, Baez GM, Garcia-Guerra A, Toledo MZ, Monteiro PL, Melo LF, Ochoa JC, Santos JE, Sartori R. Pivotal periods for pregnancy loss during the first trimester of gestation in lactating dairy cows. Theriogenology 2016; 86:239-253.
6. Wilmut I, Sales DI, Ashworth CJ. Maternal and embryonic factors associated with prenatal loss in mammals. J Reprod Fertil 1986; 76:851-864.
7. Spencer TE, Bazer FW. Ovine interferon tau suppresses transcription of the estrogen receptor and oxytocin receptor genes in the ovine endometrium. Endocrinology 1996; 137:1144-1147.
8. Spencer TE, Bazer FW. Biology of progesterone action during pregnancy recognition and maintenance of pregnancy. Front Biosci 2002; 7:d1879-1898.
9. Spencer TE, Sandra O, Wolf E. Genes involved in conceptus-endometrial interactions in ruminants: insights from reductionism and thoughts on holistic approaches. Reproduction 2008; 135:165-179.
10. Northey DL, French LR. Effect of embryo removal and intrauterine infusion of embryonic homogenates on the lifespan of the bovine corpus luteum. J Anim Sci 1980; 50:298-302.
11. Rizos D, Scully S, Kelly AK, Ealy AD, Moros R, Duffy P, Al Naib A, Forde N, Lonergan P. Effects of human chorionic gonadotrophin administration on day 5 after oestrus on corpus luteum characteristics, circulating progesterone and conceptus elongation in cattle. Reprod Fertil Dev 2012; 24:472-481.
12. Negrón-Pérez VM, Zhang Y, Hansen PJ. Single-cell gene expression of the bovine blastocyst. Reproduction 2017; 154:627-644.
13. Kelleher AM, DeMayo FJ, Spencer TE. Uterine Glands: Developmental Biology and Functional Roles in Pregnancy. Endocr Rev 2019; 40:1424-1445.
14. Simintiras CA, Sánchez JM, McDonald M, Lonergan P. Progesterone alters the bovine uterine fluid lipidome during the period of elongation. Reproduction 2019; 157:399-411.
15. Simintiras CA, Sánchez JM, McDonald M, Martins T, Binelli M, Lonergan P. Biochemical characterization of progesterone-induced alterations in bovine uterine fluid amino acid and carbohydrate composition during the conceptus elongation window†. Biol Reprod 2019; 100:672-685.

16. Brooks K, Burns G, Spencer TE. Conceptus elongation in ruminants: roles of progesterone, prostaglandin, interferon tau and cortisol. J Anim Sci Biotechnol 2014; 5:53.
17. Spencer TE, Forde N, Lonergan P. The role of progesterone and conceptus-derived factors in uterine biology during early pregnancy in ruminants. J Dairy Sci 2016; 99:5941-5950.
18. Forde N, Bazer FW, Spencer TE, Lonergan P. 'Conceptualizing' the Endometrium: Identification of Conceptus-Derived Proteins During Early Pregnancy in Cattle. Biol Reprod 2015; 92:156.
19. Platanias LC. Mechanisms of type-I- and type-II-interferon-mediated signalling. Nat Rev Immunol 2005; 5:375-386.
20. Kim S, Choi Y, Bazer FW, Spencer TE. Identification of genes in the ovine endometrium regulated by interferon tau independent of signal transducer and activator of transcription 1. Endocrinology 2003; 144:5203-5214.
21. Choi Y, Johnson GA, Burghardt RC, Berghman LR, Joyce MM, Taylor KM, Stewart MD, Bazer FW, Spencer TE. Interferon regulatory factor-two restricts expression of interferon-stimulated genes to the endometrial stroma and glandular epithelium of the ovine uterus. Biol Reprod 2001; 65:1038-1049.
22. Bazer FW. Pregnancy recognition signaling mechanisms in ruminants and pigs. J Anim Sci Biotechnol 2013; 4:23.
23. Bazer FW, Thatcher WW. Chronicling the discovery of interferon tau. Reproduction 2017; 154:F11-F20.
24. Forde N, Lonergan P. Transcriptomic analysis of the bovine endometrium: What is required to establish uterine receptivity to implantation in cattle? J Reprod Dev 2012; 58:189-195.
25. Bazer FW, Wu G, Spencer TE, Johnson GA, Burghardt RC, Bayless K. Novel pathways for implantation and establishment and maintenance of pregnancy in mammals. Mol Hum Reprod 2010; 16:135-152.
26. Joyce MM, Burghardt JR, Burghardt RC, Hooper RN, Jaeger LA, Spencer TE, Bazer FW, Johnson GA. Pig conceptuses increase uterine interferon-regulatory factor 1 (IRF1), but restrict expression to stroma through estrogen-induced IRF2 in luminal epithelium. Biol Reprod 2007; 77:292-302.
27. Joyce MM, Burghardt JR, Burghardt RC, Hooper RN, Bazer FW, Johnson GA. Uterine MHC class I molecules and beta 2-microglobulin are regulated by progesterone and conceptus interferons during pig pregnancy. J Immunol 2008; 181:2494-2505.
28. Mathew DJ, Lucy MC, D Geisert R. Interleukins, interferons, and establishment of pregnancy in pigs. Reproduction 2016; 151:R111-122.
29. Kim M, Seo H, Choi Y, Shim J, Bazer FW, Ka H. Swine leukocyte antigen-DQ expression and its regulation by interferon-gamma at the maternal-fetal interface in pigs. Biol Reprod 2012; 86:43.
30. Mathew DJ, Sánchez JM, Passaro C, Charpigny G, Behura SK, Spencer TE, Lonergan P. Interferon tau-dependent and independent effects of the bovine conceptus on the endometrial transcriptome†. Biol Reprod 2019; 100:365-380.

31. Ireland JJ, Murphee RL, Coulson PB. Accuracy of predicting stages of bovine estrous cycle by gross appearance of the corpus luteum. J Dairy Sci 1980; 63:155-160.
32. MacKintosh SB, Schuberth HJ, Healy LL, Sheldon IM. Polarised bovine endometrial epithelial cells vectorially secrete prostaglandins and chemotactic factors under physiological and pathological conditions. Reproduction 2013; 145:57-72.
33. Turner ML, Cronin JG, Healey GD, Sheldon IM. Epithelial and stromal cells of bovine endometrium have roles in innate immunity and initiate inflammatory responses to bacterial lipopeptides in vitro via Toll-like receptors TLR2, TLR1, and TLR6. Endocrinology 2014; 155:1453-1465.
34. Healy LL, Cronin JG, Sheldon IM. Polarized Epithelial Cells Secrete Interleukin 6 Apically in the Bovine Endometrium. Biol Reprod 2015; 92:151.
35. Li X, Li Z, Hou D, Zhao Y, Wang C. The bovine endometrial epithelial cells promote the differentiation of trophoblast stem-like cells to binucleate trophoblast cells. Cytotechnology 2016; 68:2687-2698.
36. Jackson C, Neville T, Mercadante V, Waters K, Lamb G, Dahlen C, Redden R. Efficacy of various five-day estrous synchronization protocols in sheep. Small Ruminant Research 2014; 120:100-107.
37. Moraes JGN, Behura SK, Geary TW, Hansen PJ, Neibergs HL, Spencer TE. Uterine influences on conceptus development in fertility-classified animals. Proc Natl Acad Sci U S A 2018; 115:E1749-E1758.
38. Bolger AM, Lohse M, Usadel B. Trimmomatic: a flexible trimmer for Illumina sequence data. Bioinformatics 2014; 30:2114-2120.
39. Kim D, Langmead B, Salzberg SL. HISAT: a fast spliced aligner with low memory requirements. Nat Methods 2015; 12:357-360.
40. Liao Y, Smyth GK, Shi W. featureCounts: an efficient general purpose program for assigning sequence reads to genomic features. Bioinformatics 2014; 30:923-930.
41. Zhou X, Lindsay H, Robinson MD. Robustly detecting differential expression in RNA sequencing data using observation weights. Nucleic Acids Res 2014; 42:e91.
42. Huang dW, Sherman BT, Lempicki RA. Systematic and integrative analysis of large gene lists using DAVID bioinformatics resources. Nat Protoc 2009; 4:44-57.
43. Goossens K, Van Poucke M, Van Soom A, Vandesompele J, Van Zeveren A, Peelman LJ. Selection of reference genes for quantitative real-time PCR in bovine preimplantation embryos. BMC Dev Biol 2005; 5:27.
44. Hellemans J, Mortier G, De Paepe A, Speleman F, Vandesompele J. qBase relative quantification framework and software for management and automated analysis of real-time quantitative PCR data. Genome Biol 2007; 8:R19.
45. Vandesompele J, De Preter K, Pattyn F, Poppe B, Van Roy N, De Paepe A, Speleman F. Accurate normalization of real-time quantitative RT-PCR data by geometric averaging of multiple internal control genes. Genome Biol 2002; 3:RESEARCH0034.
46. Herath S, Fischer DP, Werling D, Williams EJ, Lilly ST, Dobson H, Bryant CE, Sheldon IM. Expression and function of Toll-like receptor 4 in the endometrial cells of the uterus. Endocrinology 2006; 147:562-570.

47. Niu J, Chang Z, Peng B, Xia Q, Lu W, Huang P, Tsao MS, Chiao PJ. Keratinocyte growth factor/fibroblast growth factor-7-regulated cell migration and invasion through activation of NF-kappaB transcription factors. J Biol Chem 2007; 282:6001-6011.
48. Chen C, Spencer TE, Bazer FW. Fibroblast growth factor-10: a stromal mediator of epithelial function in the ovine uterus. Biol Reprod 2000; 63:959-966.
49. Koji T, Chedid M, Rubin JS, Slayden OD, Csaky KG, Aaronson SA, Brenner RM. Progesterone-dependent expression of keratinocyte growth factor mRNA in stromal cells of the primate endometrium: keratinocyte growth factor as a progestomedin. J Cell Biol 1994; 125:393-401.
50. Cooke FN, Pennington KA, Yang Q, Ealy AD. Several fibroblast growth factors are expressed during pre-attachment bovine conceptus development and regulate interferon-tau expression from trophectoderm. Reproduction 2009; 137:259-269.
51. Hashizume K, Shimada A, Nakano H, Takahashi T. Bovine trophoblast cell culture systems: a technique to culture bovine trophoblast cells without feeder cells. Methods Mol Med 2006; 121:179-188.
52. Ka H, Jaeger LA, Johnson GA, Spencer TE, Bazer FW. Keratinocyte growth factor is up-regulated by estrogen in the porcine uterine endometrium and functions in trophectoderm cell proliferation and differentiation. Endocrinology 2001; 142:2303-2310.
53. Metzemaekers M, Vanheule V, Janssens R, Struyf S, Proost P. Overview of the Mechanisms that May Contribute to the Non-Redundant Activities of Interferon-Inducible CXC Chemokine Receptor 3 Ligands. Front Immunol 2017; 8:1970.
54. Zhang X, Chen L, Dang WQ, Cao MF, Xiao JF, Lv SQ, Jiang WJ, Yao XH, Lu HM, Miao JY, Wang Y, Yu SC, et al. CCL8 secreted by tumor-associated macrophages promotes invasion and stemness of glioblastoma cells via ERK1/2 signaling. Lab Invest 2020; 100:619-629.
55. Sakumoto R, Hayashi KG, Fujii S, Kanahara H, Hosoe M, Furusawa T, Kizaki K. Possible Roles of CC- and CXC-Chemokines in Regulating Bovine Endometrial Function during Early Pregnancy. Int J Mol Sci 2017; 18.
56. Song W, Li D, Tao L, Luo Q, Chen L. Solute carrier transporters: the metabolic gatekeepers of immune cells. Acta Pharm Sin B 2020; 10:61-78.
57. González-Navajas JM, Lee J, David M, Raz E. Immunomodulatory functions of type I interferons. Nat Rev Immunol 2012; 12:125-135.
58. Ivashkiv LB, Donlin LT. Regulation of type I interferon responses. Nat Rev Immunol 2014; 14:36-49.
59. Antonczyk A, Krist B, Sajek M, Michalska A, Piaszyk-Borychowska A, Plens-Galaska M, Wesoly J, Bluyssen HAR. Direct Inhibition of IRF-Dependent Transcriptional Regulatory Mechanisms Associated With Disease. Front Immunol 2019; 10:1176.
60. Fleming JG, Spencer TE, Safe SH, Bazer FW. Estrogen regulates transcription of the ovine oxytocin receptor gene through GC-rich SP1 promoter elements. Endocrinology 2006; 147:899-911.
61. Robinson RS, Mann GE, Lamming GE, Wathes DC. The effect of pregnancy on the expression of uterine oxytocin, oestrogen and progesterone receptors during early pregnancy in the cow. J Endocrinol 1999; 160:21-33.

62. Telgmann R, Bathgate R, Jaeger S, Tillmann G, Ivell R. Transcriptional regulation of the bovine oxytocin receptor gene. Biology of Reproduction 2003; 68:1015-1026.
63. Forde N, Carter F, Spencer TE, Bazer FW, Sandra O, Mansouri-Attia N, Okumu LA, McGettigan PA, Mehta JP, McBride R, O'Gaora P, Roche JF, et al. Conceptus-induced changes in the endometrial transcriptome: how soon does the cow know she is pregnant? Biol Reprod 2011; 85:144-156.
64. Hansen TR, Sinedino LDP, Spencer TE. Paracrine and endocrine actions of interferon tau (IFNT). Reproduction 2017; 154:F45-F59.
65. Betancor G, Dicks MDJ, Jimenez-Guardeño JM, Ali NH, Apolonia L, Malim MH. The GTPase Domain of MX2 Interacts with the HIV-1 Capsid, Enabling Its Short Isoform to Moderate Antiviral Restriction. Cell Rep 2019; 29:1923-1933.e1923.
66. Green JC, Okamura CS, Poock SE, Lucy MC. Measurement of interferon-tau (IFN-tau) stimulated gene expression in blood leukocytes for pregnancy diagnosis within 18-20d after insemination in dairy cattle. Anim Reprod Sci 2010; 121:24-33.
67. Babiker HA, Saito T, Nakatsu Y, Takasuga S, Morita M, Sugimoto Y, Ueda J, Watanabe T. Molecular cloning, polymorphism, and functional activity of the bovine and water buffalo. Springerplus 2016; 5:2109.
68. Klein C, Bauersachs S, Ulbrich SE, Einspanier R, Meyer HH, Schmidt SE, Reichenbach HD, Vermehren M, Sinowatz F, Blum H, Wolf E. Monozygotic twin model reveals novel embryo-induced transcriptome changes of bovine endometrium in the preattachment period. Biol Reprod 2006; 74:253-264.
69. Gray CA, Abbey CA, Beremand PD, Choi Y, Farmer JL, Adelson DL, Thomas TL, Bazer FW, Spencer TE. Identification of endometrial genes regulated by early pregnancy, progesterone, and interferon tau in the ovine uterus. Biol Reprod 2006; 74:383-394.
70. Fleming JA, Choi Y, Johnson GA, Spencer TE, Bazer FW. Cloning of the ovine estrogen receptor-alpha promoter and functional regulation by ovine interferon-tau. Endocrinology 2001; 142:2879-2887.
71. Perry DJ, Austin KJ, Hansen TR. Cloning of interferon-stimulated gene 17: the promoter and nuclear proteins that regulate transcription. Mol Endocrinol 1999; 13:1197-1206.
72. Mathew DJ, Newsom EM, Guyton JM, Tuggle CK, Geisert RD, Lucy MC. Activation of the transcription factor nuclear factor-kappa B in uterine luminal epithelial cells by interleukin 1 Beta 2: a novel interleukin 1 expressed by the elongating pig conceptus. Biol Reprod 2015; 92:107.
73. Platanitis E, Decker T. Regulatory Networks Involving STATs, IRFs, and NFκB in Inflammation. Front Immunol 2018; 9:2542.
74. Iwanaszko M, Kimmel M. NF-κB and IRF pathways: cross-regulation on target genes promoter level. BMC Genomics 2015; 16:307.
75. Roy S, Guler R, Parihar SP, Schmeier S, Kaczkowski B, Nishimura H, Shin JW, Negishi Y, Ozturk M, Hurdayal R, Kubosaki A, Kimura Y, et al. Batf2/Irf1 induces inflammatory responses in classically activated macrophages, lipopolysaccharides, and mycobacterial infection. J Immunol 2015; 194:6035-6044.
76. Kanemaru H, Yamane F, Fukushima K, Matsuki T, Kawasaki T, Ebina I, Kuniyoshi K, Tanaka H, Maruyama K, Maeda K, Satoh T, Akira S. Antitumor effect of. Proc Natl Acad Sci U S A 2017; 114:E7331-E7340.

77. Guler R, Roy S, Suzuki H, Brombacher F. Targeting Batf2 for infectious diseases and cancer. Oncotarget 2015; 6:26575-26582.
78. Verma S, Pal R, Gupta SK. Decrease in invasion of HTR-8/SVneo trophoblastic cells by interferon gamma involves cross-communication of STAT1 and BATF2 that regulates the expression of JUN. Cell Adh Migr 2018; 12:432-446.
79. Hediger MA, Clémençon B, Burrier RE, Bruford EA. The ABCs of membrane transporters in health and disease (SLC series): introduction. Mol Aspects Med 2013; 34:95-107.
80. Gao H, Wu G, Spencer TE, Johnson GA, Bazer FW. Select nutrients in the ovine uterine lumen. III. Cationic amino acid transporters in the ovine uterus and peri-implantation conceptuses. Biol Reprod 2009; 80:602-609.
81. Gao H, Wu G, Spencer TE, Johnson GA, Bazer FW. Select nutrients in the ovine uterine lumen. IV. Expression of neutral and acidic amino acid transporters in ovine uteri and peri-implantation conceptuses. Biol Reprod 2009; 80:1196-1208.
82. Godkin JD, Smith SE, Johnson RD, Doré JJ. The role of trophoblast interferons in the maintenance of early pregnancy in ruminants. Am J Reprod Immunol 1997; 37:137-143.
83. Groebner AE, Rubio-Aliaga I, Schulke K, Reichenbach HD, Daniel H, Wolf E, Meyer HH, Ulbrich SE. Increase of essential amino acids in the bovine uterine lumen during preimplantation development. Reproduction 2011; 141:685-695.
84. Gwatkin RB. Defined media and development of mammalian eggs in vitro. Ann N Y Acad Sci 1966; 139:79-90.
85. Forde N, Simintiras CA, Sturmey R, Mamo S, Kelly AK, Spencer TE, Bazer FW, Lonergan P. Amino acids in the uterine luminal fluid reflects the temporal changes in transporter expression in the endometrium and conceptus during early pregnancy in cattle. PLoS One 2014; 9:e100010.
86. Ruprecht JJ, Kunji ERS. The SLC25 Mitochondrial Carrier Family: Structure and Mechanism. Trends Biochem Sci 2020; 45:244-258.
87. Ren L, Wang Z, An L, Zhang Z, Tan K, Miao K, Tao L, Cheng L, Yang M, Wu Z, Tian J. Dynamic comparisons of high-resolution expression profiles highlighting mitochondria-related genes between in vivo and in vitro fertilized early mouse embryos. Hum Reprod 2015; 30:2892-2911.
88. Lindhurst MJ, Fiermonte G, Song S, Struys E, De Leonardis F, Schwartzberg PL, Chen A, Castegna A, Verhoeven N, Mathews CK, Palmieri F, Biesecker LG. Knockout of Slc25a19 causes mitochondrial thiamine pyrophosphate depletion, embryonic lethality, CNS malformations, and anemia. Proc Natl Acad Sci U S A 2006; 103:15927-15932.
89. Livingston JH, Lin JP, Dale RC, Gill D, Brogan P, Munnich A, Kurian MA, Gonzalez-Martinez V, De Goede CG, Falconer A, Forte G, Jenkinson EM, et al. A type I interferon signature identifies bilateral striatal necrosis due to mutations in ADAR1. J Med Genet 2014; 51:76-82.
90. Piekutowska-Abramczuk D, Mierzewska H, Bekiesińska-Figatowska M, Ciara E, Trubicka J, Pronicki M, Rokicki D, Rydzanicz M, Płoski R, Pronicka E. Bilateral striatal necrosis caused by ADAR mutations in two siblings with dystonia and freckles-like skin changes that should be differentiated from Leigh syndrome. Folia Neuropathol 2016; 54:405-409.

91. Shaw GC, Cope JJ, Li L, Corson K, Hersey C, Ackermann GE, Gwynn B, Lambert AJ, Wingert RA, Traver D, Trede NS, Barut BA, et al. Mitoferrin is essential for erythroid iron assimilation. Nature 2006; 440:96-100.
92. Gorgoglione R, Porcelli V, Santoro A, Daddabbo L, Vozza A, Monné M, Di Noia MA, Palmieri L, Fiermonte G, Palmieri F. The human uncoupling proteins 5 and 6 (UCP5/SLC25A14 and UCP6/SLC25A30) transport sulfur oxyanions, phosphate and dicarboxylates. Biochim Biophys Acta Bioenerg 2019; 1860:724-733.
93. Tríbulo P, Balzano-Nogueira L, Conesa A, Siqueira LG, Hansen PJ. Changes in the uterine metabolome of the cow during the first 7 days after estrus. Mol Reprod Dev 2019; 86:75-87.
94. Kane M, Zang TM, Rihn SJ, Zhang F, Kueck T, Alim M, Schoggins J, Rice CM, Wilson SJ, Bieniasz PD. Identification of Interferon-Stimulated Genes with Antiretroviral Activity. Cell Host Microbe 2016; 20:392-405.
95. Yin Y, Li Y, Zhang W. The growth hormone secretagogue receptor: its intracellular signaling and regulation. Int J Mol Sci 2014; 15:4837-4855.
96. Martin JR, Lieber SB, McGrath J, Shanabrough M, Horvath TL, Taylor HS. Maternal ghrelin deficiency compromises reproduction in female progeny through altered uterine developmental programming. Endocrinology 2011; 152:2060-2066.
97. Luque EM, Torres PJ, de Loredo N, Vincenti LM, Stutz G, Santillán ME, Ruiz RD, de Cuneo MF, Martini AC. Role of ghrelin in fertilization, early embryo development, and implantation periods. Reproduction 2014; 148:159-167.
98. Aghajanova L, Rumman A, Altmäe S, Wånggren K, Stavreus-Evers A. Diminished endometrial expression of ghrelin and ghrelin receptor contributes to infertility. Reprod Sci 2010; 17:823-832.
99. Deaver SE, Hoyer PB, Dial SM, Field ME, Collier RJ, Rhoads ML. Localization of ghrelin and its receptor in the reproductive tract of Holstein heifers. J Dairy Sci 2013; 96:150-157.
100. Dovolou E, Periquesta E, Messinis IE, Tsiligianni T, Dafopoulos K, Gutierrez-Adan A, Amiridis GS. Daily supplementation with ghrelin improves in vitro bovine blastocysts formation rate and alters gene expression related to embryo quality. Theriogenology 2014; 81:565-571.
101. Kerns JA, Emerman M, Malik HS. Positive selection and increased antiviral activity associated with the PARP-containing isoform of human zinc-finger antiviral protein. PLoS Genet 2008; 4:e21.
102. Cagliani R, Guerini FR, Fumagalli M, Riva S, Agliardi C, Galimberti D, Pozzoli U, Goris A, Dubois B, Fenoglio C, Forni D, Sanna S, et al. A trans-specific polymorphism in ZC3HAV1 is maintained by long-standing balancing selection and may confer susceptibility to multiple sclerosis. Mol Biol Evol 2012; 29:1599-1613.
103. Todorova T, Bock FJ, Chang P. Poly(ADP-ribose) polymerase-13 and RNA regulation in immunity and cancer. Trends Mol Med 2015; 21:373-384.
104. Evans GE, Martínez-Conejero JA, Phillipson GT, Sykes PH, Sin IL, Lam EY, Print CG, Horcajadas JA, Evans JJ. In the secretory endometria of women, luminal epithelia exhibit gene and protein expressions that differ from those of glandular epithelia. Fertil Steril 2014; 102:307-317.e307.

105. Ozawa M, Sakatani M, Yao J, Shanker S, Yu F, Yamashita R, Wakabayashi S, Nakai K, Dobbs KB, Sudano MJ, Farmerie WG, Hansen PJ. Global gene expression of the inner cell mass and trophectoderm of the bovine blastocyst. BMC Dev Biol 2012; 12:33.
106. Wang X, Ao H, Song M, Bai L, He W, Wang C, Yu Y. Identification of DNA methylation regulated novel host genes relevant to inhibition of virus replication in porcine PK15 cell using double stranded RNA mimics and DNA methyltransferase inhibitor. Genomics 2019; 111:1464-1473.
107. Black SG, Arnaud F, Palmarini M, Spencer TE. Endogenous retroviruses in trophoblast differentiation and placental development. Am J Reprod Immunol 2010; 64:255-264.
108. Haig D. Retroviruses and the placenta. Curr Biol 2012; 22:R609-613.
109. Cornelis G, Heidmann O, Degrelle SA, Vernochet C, Lavialle C, Letzelter C, Bernard-Stoecklin S, Hassanin A, Mulot B, Guillomot M, Hue I, Heidmann T, et al. Captured retroviral envelope syncytin gene associated with the unique placental structure of higher ruminants. Proc Natl Acad Sci U S A 2013; 110:E828-837.
110. Denner J. Expression and function of endogenous retroviruses in the placenta. APMIS 2016; 124:31-43.
111. Black SG, Arnaud F, Burghardt RC, Satterfield MC, Fleming JA, Long CR, Hanna C, Murphy L, Biek R, Palmarini M, Spencer TE. Viral particles of endogenous betaretroviruses are released in the sheep uterus and infect the conceptus trophectoderm in a transspecies embryo transfer model. J Virol 2010; 84:9078-9085.
112. Dunlap KA, Palmarini M, Varela M, Burghardt RC, Hayashi K, Farmer JL, Spencer TE. Endogenous retroviruses regulate periimplantation placental growth and differentiation. Proc Natl Acad Sci U S A 2006; 103:14390-14395.
113. Ruiz-González I, Xu J, Wang X, Burghardt RC, Dunlap KA, Bazer FW. Exosomes, endogenous retroviruses and toll-like receptors: pregnancy recognition in ewes. Reproduction 2015; 149:281-291.
114. Nakaya Y, Miyazawa T. The Roles of Syncytin-Like Proteins in Ruminant Placentation. Viruses 2015; 7:2928-2942.
115. McLean KJ, Crouse MS, Crosswhite MR, Black DN, Dahlen CR, Borowicz PP, Reynolds LP, Ward AK, Neville BW, Caton JS. Endogenous retroviral gene elements (Transl Anim Sci 2017; 1:239-249.
116. Passaro C, Tutt D, Mathew DJ, Sanchez JM, Browne JA, Boe-Hansen GB, Fair T, Lonergan P. Blastocyst-induced changes in the bovine endometrial transcriptome. Reproduction 2018; 156:219-229.
117. Weiner CM, Smirnova NP, Webb BT, Van Campen H, Hansen TR. Interferon stimulated genes, CXCR4 and immune cell responses in peripheral blood mononuclear cells infected with bovine viral diarrhea virus. Res Vet Sci 2012; 93:1081-1088.

Table 1. GenBank accession number, gene name, primer direction, primer sequence, product size, percent amplification efficiency, and source of primer of cDNAs amplified during real-time quantitative PCR (RT-qPCR). Primers sequences were previously published or designed using Primer3Plus (P3P; Version 2.4.2).

GenBank Acc. Number	Gene	Primer	Primer Sequence (5'-3')	Product Size (bp)	Amp. E. (%)	Source
NM_178320	*PPIA*	Forward	CATACAGGTCCTGGCATCTTGTCC	108	--	[116]
		Reverse	CACGTGCTTGCCATCCAACC			
NM_174178	*SDHA*	Forward	ACTTCACCGTTGATGGCAA	59	--	[116]
		Reverse	GCAGAAATCGCATCTGAAA			
NM_001077953.1	*RNF11*	Forward	TCCGGGAGTGTGTGATCTGTATGAT	131	--	[30]
		Reverse	GCAGGAGGGGCACGTGAAGG			
XM_010801645.3	*MX1*	Forward	CGAGCCGAGTTCTCCAAATG	114	96	[116]
		Reverse	CAACTCTCTGCCACGATACC			
NM_001077900.1	*STAT1*	Forward	GCATTAGTCAGGGCCCAAATTGTTACAG	139	96	[116]
		Reverse	GCCAGATACAGGAAGCTTTGCAC			
NM_173941.2	*MX2*	Forward	GGGCAGCGGAATCATCACCCG	102	93	[30]
		Reverse	AGCTGCTGCGTAATGTTGCGGTA			
NM_001015570.3	*LGALS9*	Forward	TCAGCTTCCAGCCTCCAGGG	86	97	[116]
		Reverse	TCCAGGGGCGCTGTGTATGGT			
NM_001046316.2	*LGALS3BP*	Forward	CAACTGCAGACACGACAAGG	88	95	[116]
		Reverse	AGGGATTTCGCCAGATAGGT			
NM_174301.3	*CXCR4*	Forward	AAGGCTCAGAAGCGCAAG	102	102	[117]
		Reverse	GAGTCGATGCTGATCCCAAT			
NM_174366.1	*ISG15*	Forward	CCAACCAGTGTCTGCAGAGA	76	97	[30]
		Reverse	CCCTAGCATCTTCACCGTCA			
NM_001024557.1	*OAS2*	Forward	TGGATAACACCTGCTGGCTG	82	93	P3P
		Reverse	GGTCCAGGTGACTCGTTCTG			
NM_001101866.2	*IDO1*	Forward	CACCCCAAAGAAGTTTGCCG	80	99	P3P
		Reverse	GCTGAATGCCCAGGAGAACA			
NM_001114506.1	*TNFSF13B*	Forward	GGGACGAACTGAGTCTGGTG	147	96	P3P
		Reverse	TCTTAGCATCTTCCCGGGGT			
XM_005216258.4	*MAP6*	Forward	ATAAGCCAACCCCAGCTGAC	82	110	P3P
		Reverse	GGAGGTTCCTTGAAGGGCTC			
NM_001192561.2	*BATF2*	Forward	ATCTCCTGCACAGCTGTCAC	132	106	P3P
		Reverse	AGGAACTCTAGAGGGGCAGG			
XM_003586006.5	*ZC3HAV1*	Forward	AGGCCTTTTGTGACCCCAAA	119	97	P3P
		Reverse	TGTGACGGATGAAGGTGTGG			
XM_015475541.2	*LIF*	Forward	GGGACAACTCAACAGCAGTG	91	96	P3P
		Reverse	GCACAGCTTGTCCAGGTTG			

Table 2. Genes up- or down-regulated in the Venn diagram (Figure 4).

I					II		III
Up	HSH2D	IRF3	HEATR5B	POLH	**Up**	DTX3L	**Up**
GBP2	OPTN	TAP2	IRF2	TRIM38	MX2	PML	ZC3HAV1
GBP6	DAXX	CMTR1	FAM111B	C2	IFIT3	TRIM5	
SLFN11	ATXN3	PAPD4	JADE2	ARSH	RSAD2	IRF9	
IDO1	GNB4	SCLY	DUSP11	XRN2	IFIT1	IRF7	
IFITM3	RBCK1	NT5C3A	YTHDC2	ELMO2	IFI44	TIFA	
ACKR4	NMI	CDKN2AIP	TMEM268	IRF1	IFIT2	XAF1	
TNFSF13B	PLSCR2	RAB8B	CHMP5	RAB37	ISG15	PARP12	
MLKL	GDAP2	ZNF607	PLSCR4	TMEM106A	GBP4	IFIT5	
MASTL	MOV10	OGFR	CTC1	TREX1	IFI44L	PARP10	
SP110	STAT1	PSME2	XPO1	DDX19B	SAMD9	PNPT1	
KIF5C	ATAD1	ANKFY1	RBMS2		OAS2	SLC15A3	
IFITM1	LGALS3BP	PXK	NFE2L3		BST2	FAM3B	
WARS	AKAP7	PSMA2	MAT2B		UBA7	IFI16	
FOXS1	USP25	LAP3	TAPBPL		USP18	SP140	
ISG20	ANXA1	DNAJC1	PRICKLE3		ZBP1	TRANK1	
GNGT2	SLC25A28	SLC25A30	NUB1		OAS1X	ADAR	
SLFN12	PARM1	SERTAD1	DNPEP		MX1	PLEKHA4	
APOL3	NCOA7	ERAP1	KIFC3		GBP1	TRIM34	
TMEM140	VCPIP1	RIPK3	CD47		CMPK2	CMTR2	
CDADC1	TRIM56	STK38L	RNF139		RTP4	TDRD7	**IV**
CD274	GRINA	TAPBP	B2M		RNF213	LGALS9	**Up**
GHSR	SPATS2L	CUL4B	KAT2A		BATF2	PARP9	OAS1Z
HES4	ATP10A	NR3C1	AZI2		EPSTI1	IFI6	LOC112441507
CASP4	NLRC5	RNF19B	MCHR1		DDX58	RBM43	OAS1Y
BCL2L15	CNP	AIDA	MITD1		PARP14	UBE2L6	CCDC194
DRAM1	CBLN3	RBBP6	TLR3		TNFSF10	RNASEL	SP140L
IFI35	ATP8B4	RNF31	CASP8		HERC6	TRIM21	LOC107132617
FAM212A	MAD2L2	PAPD7	FBXO33		IFIH1	N4BP1	CGAS
BOLA-DMB	PSMB9	SLC25A19	RICTOR		GBP5	TAP1	C7H19orf66
SASS6	BCL2L12	CCDC82	ABHD1		HERC5	TRIM25	LOC112446427
BPNT1	BCL2L14	IL15RA	RNF114		PLAC8	DHX58	TMPRSS2
MORC3	PSMB8	TRIM26	SHISA5		ZNFX1	CASP7	
GTF2B	PSMF1	CCDC6	PLEKHA7		EIF2AK2	IFI27	
STAT2	LEKR1	TRIM16	CDK18		SP100		
IRF8	NAMPT	PPP2R3C	PDCD4		IRF4		

V			
Up	C3AR1	DYNC1H1	ABCB7
CLEC4F	PTPRO	RAPGEF3	DNAJC13
CCL8	C21ORF91	PARP8	GAB1
CXCL11	PDCD1	SYNE2	BID
CXCL10	CD53	PLPP3	MXD1
TIMD4	CLEC2D	LIFR	TTC9C
APOBEC3Z1	POLD3	RIPK2	PHF11
OAS1	TFEC	KYAT3	UNC93B1
GBP7	C19ORF66	ARHGEF3	LDB2
GVINP1	ABCG2	SCARF1	PSMA8
CXCL9	STARD8	ZC3H12C	PLA2G16
IFI47	MICB	ZCCHC6	CXORF21
MYADML	C3ORF38	AIFM2	UNC45B
MB21D1	HEG1	PSME1	ART3
SECTM1	IL23A	ZNF628	C1ORF115
TNFSF13BL	HORMAD1	TGM2	NCF1
ISG12B	IL15	PDE5A	IFI27L
LOR	NEURL3	MTO1	ALS2
CYP2J2	PTPN11	MRPL32	MAN1C1
TCF15	SIGLEC1	ECM1	C2ORF68
KYNU	CD40	KIAA1033	**Down**
BL37	PHACTR1	PPFIBP1	KIT
P2RY6	ACOT9	SSAT-1	CHST15
CLEC10A	TAL1	FUNDC1	FAM101B
CDHR5	FRMD4B	PPA1	PECAM1
RUBCN	ACSL5	SLK	CD93
REC8	TSKU	TOR1AIP2	AFAP1L1
C1ORF109	ADGRF5	FYTTD1	FAM124B
ZNF366	DECR2	IFRG15	APLNR
BL36	CTSS	CFLAR	SOX18
TLR4	FAM172B	PAPD5	PALD1
EHD3	C4A	VPS13C	VASH1
LPCAT2	IP6K1	JAK2	JAG1
AGRN	STOML1	TCEAL1	
REGAKINE-1	FAS	USF1	
TMEM74B	GSDMD	MIA3	
SLC2A6	TLE4	USP34	
BL37L	DYSF	SOCS2	

VI			
Up	KIF26A	TSPAN32	LOC782527
CNGB1	ABCC11	ATP8A2	WDR17
SAA4	ZC3H12D	CLEC2D11	SOCS1
LYZ3	MYAML2	GOLCA6L22	SCN9A
PRM1	LOC100141258	ERBB4	ADAM19
SOX10	IL3RA	PSCA	CYP2S1
LOC781494	ANKRD35	C5H22orf23	JPH2
JAKMIP3	LUZP2	THEM6	RAB19
NUGGC	UPB1	CHST4	KRT42
MUC12	HS3ST1	TRIM14	MYO1A
LOC511617	SLC9C1	LOC101905194	VWA5A
OASL	C1R	LOC104970178	FAM71A
BIRC7	LRIT3	TNFRSF9	ARID3C
LOC787234	PLA2G7	LOC112448863	IQCD
ADGRG7	CAPN8	DSC1	GANC
IFNL3	LOC112445995	LOC515697	COX7A1
LOC512869	BREH1	LPL	RIPOR3
BVES	SLC23A2	LOC509972	MASP1
TMPRSS5	TAGAP	LOC112446668	SIX1
TNFSF4	ARHGAP9	SCNN1B	CCDC39
SBK3	CDHR4	GMNC	SCNN1G
ASB5	ABCB5	LOC616948	ZCCHC2
CNDP1	IFITM2	SLC13A5	PMAIP1
FRAS1	CLDN16	ANKRD53	TM6SF2
ACVR1C	SULT6B1	CCDC190	EPHX2
SLCO2B1	TGM7	LOC530929	FBXO16
SLC22A10	C5	LOC101902154	PGR
OXT	MESP2	CPLX1	INPP5F
ODF3L1	CD34	LOC112444847	IQUB
DPY19L2	PDCD1LG2	ISG12B	NFIX
LOC512440	RPE65	BST1	ORC5
ELMOD1	LOC521656	TACR1	TCTN3
TRIM15	LOC512672	PLA2R1	EHD4
TRPC3	LOC101903126	OVCH1	OVOL1
GPR63	LOC101905257	LOC512323	CATSPERE
PCK1	STAT4	CSPG5	CIITA
SYT16	B3GNT3	TAF4B	RAD21L1
LOC107132327	LY6L	IL34	BTC

VI (*Continued*)							
LOC515736	C16H1orf115	RBMX2	EVA1A	CGN	SCO1	SPPL2A	**Down**
GDA	AP5B1	MST1R	C11H2orf68	HKDC1	APOPT1	PDK3	VPS33A
DUSP15	ICAM1	MUC1	PPAT	ADPGK	FPGT	ZCCHC8	MLEC
PLIN2	ICAM2	SLC27A1	BTBD11	DNAJA1	WDR18	SLC35C1	MEGF9
ZFP36	INA	UTP23	BOLA	HFE	F2R	NARS	NAV2
IL22RA1	CHST1	HK2	HACD2	RNF39	TMED8	KAT2B	UNC5B
FBXO45	TACR3	SEMA4A	ACOX3	DBNL	SCP2	DESI1	TUBB3
LOC618733	FOXQ1	FCHSD2	FBXO7	MTPAP	TCOF1	HAUS3	SAMD1
ICA1L	GABRP	LOC518495	ARL6IP5	DNMT1	MIER3	PRKAB1	BCAT1
HSPB11	THEM4	A2ML1	SARS	TPRKB	MRPL44	FGD4	ARVCF
APOBEC1	DENND2D	TRAPPC2	RFX5	EIF2AK1	RNF135	ARHGEF16	PPARA
DDIT3	GRAMD1C	LYPD6B	TAF5	SPTY2D1	DENND4C	ZMYM1	PIAS2
DRAM2	ALDH9A1	PRKAR1B	APRT	GALM	OSBPL8	CNOT9	MTFR1
FLT3LG	CROT	ZDHHC14	STXBP3	SLC1A5	SNX6	UHRF2	TUBA1A
IL18	CSRNP1	TICRR	ZNF197	COA7	CENPO	DNAJC8	PTCH1
FAM172BP	TACSTD2	TRMT13	SERINC2	TMEM255B	SEC24B	KCTD9	EML1
NKX3-1	CLDN1	CPOX	PSMB10	MTFP1	PRPSAP1	PELI1	AKAP12
LY6E	CLSTN2	ITPR2	PRKD2	PRMT9	NISCH	MCL1	LMCD1
BOLA-NC1	FAM192A	WIPF3	S1PR2	TTC4	SSBP3	FAM168B	ETV4
SFN	YARS	GIPC2	DDX24	FYB2	ANAPC11	HNRNPLL	ALDH1A3
TMEM171	FAM129A	DCK	GCHFR	TSPYL1	STRIP1	KRT7	FITM2
FUT10	AKAP6	SLC6A12	C16H1orf112	PALM	FAM110C	TRIM4	SLC25A15
PLA2G3	ZNF852	ATP7A	ELF1	SARNP	JDP2		KLF13
MISP	LIPA	TMEM41A	RRM2B	STARD3	PJA2	**Down**	SCRN1
CALCOCO2	MTR	GABARAPL1	HNF4G	DNAJC7	MARCKSL1	DESI2	FAM92A
ERAP2	SAT1	SLC25A12	TWISTNB	TXNRD1	CBLL1	MBTPS1	GVQW3
CCDC102A	TATDN3	CAMK2D	ID4	RCBTB1	STAMBP	GNPAT	PCDHA5
CSDC2	BSPRY	APOBEC3H	LOC101905041	SEPT7	KAT5	GTF2A1	ZMYND10
ZUP1	ALPK1	OSMR	B4GALT1	GYG1	ZNF710	ZDHHC23	HIST1H3A
ARL6IP1	NOSTRIN	LNPEP	EMP1	TMEM230	HGH1	PSD4	MAP6
NEB	XRCC5	TMEM144	ACSS2	NECTIN2	CEPT1	PKD1	
LOC508153	C1H3orf38	FAM76A	PCGF5	AVEN	GTPBP2	SESN3	
CTSL	SIDT2	MOCS1	ADM2	BIRC3	TIPARP	ENTR1	
WDR86	CSRNP2	UBIAD1	SNX4	MOCOS	CSTF1	NETO2	
VAMP5	LENG1	ACP2	VPS33B	GPHN	ACADM	NBEAL2	
SAMHD1	TCAF2	AP1AR	POLR2K	PLEKHO1	MTMR4	SRD5A1	

Table 3. Gene ontology enriched biological processes (BP) and kyoto encyclopedia of genes and genomes (KEGG) pathways associated with the 223 IFNT dependent epithelial (Td-Epi) DEGs (Figure 4, Regions I and II) and 70 IFNT dependent stroma fibroblast (Td-SF) DEGs (Figure 4, Regions II and III) that overlapped with the conceptus induced, IFNT dependent endometrial (CiTd-Endo) DEGs identified by Mathew et al. [30]. All DEGs were up-regulated.

Epithelial Cells		
Biological Process	**P-Value**	**Associated DEG**
Type I interferon signaling pathway	< 0.001	RNASEL, IFITM1, IFITM3, RSAD2, OAS2, IFI35, ISG20, ISG15, XAF1, MX1, MX2, SP100, BST2, STAT1, PSMB8, STAT2, IFIT3, IRF9, IFIT2, IFIT1, IFI27, IRF7, IRF8, IRF1, IRF2, IRF3, IRF4, GBP2, IFI6, ADAR
Defense response to virus	< 0.001	RNASEL, IFITM1, IFITM3, PML, TLR3, RSAD2, IFI44L, OAS2, ISG20, TRIM5, NLRC5, ISG15, MX1, MX2, DHX58, BST2, HERC5, TRIM25, IFI16, STAT1, STAT2, IRF9, IFIT3, TRIM56, IFIT2, IFIT1, TRIM34, IFIT5, IRF1, IRF3, SLFN11, EIF2AK2, GBP1, ADAR
Interferon-gamma-mediated signaling pathway	< 0.001	SP100, NMI, PML, TRIM26, TRIM25, OAS2, STAT1, TRIM21, B2M, IRF9, TRIM38, TRIM5, TRIM34, IRF7, IRF8, IRF1, IRF2, IRF3, IRF4, GBP2, GBP1
Response to virus	< 0.001	IFIH1, BST2, IFITM1, IFITM3, RSAD2, IFI44, OAS2, ISG20, DDX58, PSMA2, IFIT3, IFIT2, IFIT1, IRF7, EIF2AK2, MX1, MX2, DHX58, ADAR
Negative regulation of viral genome replication	< 0.001	RNASEL, IFITM1, BST2, IFITM3, RSAD2, PARP10, IFI16, ISG20, IFIT1, ISG15, EIF2AK2, MX1, ADAR
Negative regulation of type I interferon production	< 0.001	DDX58, NLRC5, IFIH1, ISG15, HERC5, UBA7, UBE2L6, TRIM25, IRF3, DHX58
Innate immune response	< 0.001	IFIH1, BST2, ANXA1, PML, HERC5, TLR3, TRIM26, TRIM25, IFI16, TRIM21, B2M, DDX58, NLRC5, TRIM5, CASP4, IFIT5, IRF7, C2, EIF2AK2, MX1, MX2, DHX58, ADAR, ZBP1
Protein polyubiquitination	< 0.001	DTX3L, HERC6, HERC5, RBBP6, RNF213, TRIM21, PSMB8, PSMB9, PSMA2, PSMF1, RNF114, PSME2, RNF139, RBCK1, RNF19B, RNF31
Response to interferon-alpha	< 0.001	BST2, IFITM1, IFITM3, EIF2AK2, MX2, ADAR
Antigen processing and presentation of endogenous peptide antigen via MHC class I	< 0.001	TAP2, TAP1, ERAP1, TAPBP, B2M
Response to interferon-beta	< 0.001	BST2, IFITM1, IFITM3, XAF1, STAT1

Positive regulation of I-kappaB kinase/NF-kappaB signaling	< 0.001	TRIM5, APOL3, TRIM38, TNFSF10, BST2, CASP8, SHISA5, RBCK1, TRIM25, IRF3, LGALS9, RNF31
Response to interferon-gamma	< 0.001	SP100, BST2, IFITM1, NUB1, IFITM3, TRIM21
Positive regulation of interferon-beta production	< 0.001	DDX58, IFIH1, IRF7, IRF1, TLR3, IRF3
Negative regulation of viral release from host cell	< 0.001	TRIM5, PML, TRIM26, TRIM25, TRIM21
ISG15-protein conjugation	< 0.001	ISG15, HERC5, UBA7, UBE2L6

KEGG Pathway	P-Value	Associated DEG
Influenza A	< 0.001	XPO1, IFIH1, RNASEL, PML, TLR3, RSAD2, TRIM25, OAS2, STAT1, STAT2, DDX58, IRF9, TNFSF10, IRF7, IRF3, EIF2AK2, MX1, ADAR
Herpes simplex infection	< 0.001	RNASEL, IFIH1, SP100, PML, TLR3, OAS2, STAT1, DAXX, STAT2, DDX58, IRF9, IFIT1, IRF7, TAP2, CASP8, TAP1, IRF3,
Hepatitis C	< 0.001	DDX58, IRF9, RNASEL, IFIT1, IRF7, IRF1, TLR3, IRF3, OAS2, EIF2AK2, STAT1, STAT2
Measles	< 0.001	DDX58, IRF9, IFIH1, TNFSF10, IRF7, IRF3, OAS2, EIF2AK2, MX1, STAT1, STAT2, ADAR
RIG-I-like receptor signaling pathway	< 0.001	DDX58, IFIH1, ISG15, IRF7, CASP8, TRIM25, IRF3, AZI2, DHX58

Fibroblast Cells

Biological Pathways	P-Value	Associated DEG
Defense response to virus	< 0.001	RNASEL, ZC3HAV1, BST2, PML, HERC5, RSAD2, TRIM25, IFI44L, OAS2, IFI16, IRF9, IFIT3, IFIT2, TRIM5, IFIT1, ISG15, TRIM34, IFIT5, EIF2AK2, MX1, MX2, DHX58, GBP1, ADAR
Type I interferon signaling pathway	< 0.001	RNASEL, SP100, BST2, RSAD2, OAS2, IRF9, IFIT3, IFIT2, IFIT1, IFI27, ISG15, IRF7, IRF4, XAF1, MX1, MX2, IFI6, ADAR
Response to virus	< 0.001	IFIH1, BST2, ZC3HAV1, RSAD2, IFI44, OAS2, DDX58, IFIT3, IFIT2, IFIT1, IRF7, EIF2AK2, MX1, MX2, DHX58, ADAR
Negative regulation of viral genome replication	< 0.001	RNASEL, IFIT1, ISG15, ZC3HAV1, BST2, RSAD2, IFI16, PARP10, EIF2AK2, MX1, ADAR
Interferon-gamma-mediated signaling pathway	< 0.001	IRF9, TRIM5, SP100, TRIM34, IRF7, PML, TRIM25, OAS2, IRF4, TRIM21, GBP1

Innate immune response	< 0.001	IFIH1, BST2, ZC3HAV1, PML, HERC5, TRIM25, IFI16, TRIM21, DDX58, TRIM5, IFIT5, IRF7, EIF2AK2, MX1, MX2, DHX58, ADAR, ZBP1
Negative regulation of type I interferon production	< 0.001	DDX58, IFIH1, ISG15, HERC5, UBA7, UBE2L6, TRIM25, DHX58
ISG15-protein conjugation	< 0.001	ISG15, HERC5, UBA7, UBE2L6
Response to interferon-alpha	< 0.001	BST2, EIF2AK2, MX2, ADAR
Positive regulation of interferon-alpha production	< 0.001	DDX58, IFIH1, ZC3HAV1, IRF7
Negative regulation of viral release from host cell	< 0.001	TRIM5, PML, TRIM25, TRIM21
Positive regulation of type I interferon production	< 0.001	ZC3HAV1, IRF7, IFI16, DHX58, ZBP1

KEGG Pathways	**P-Value**	**Associated DEG**
Influenza A	< 0.001	IFIH1, RNASEL, PML, RSAD2, TRIM25, OAS2, IRF9, DDX58, TNFSF10, IRF7, EIF2AK2, MX1, ADAR
Herpes simplex infection	< 0.001	DDX58, IRF9, RNASEL, IFIT1, IFIH1, SP100, IRF7, TAP1, PML, OAS2, EIF2AK2
Measles	< 0.001	DDX58, IRF9, IFIH1, TNFSF10, IRF7, OAS2, EIF2AK2, MX1, ADAR
RIG-I-like receptor signaling pathway	< 0.001	DDX58, IFIH1, ISG15, IRF7, TRIM25, DHX58
Hepatitis C	< 0.001	DDX58, IRF9, RNASEL, IFIT1, IRF7, OAS2, EIF2AK2

Table 4. Gene name, cell type, normalized relative quantities (NRQ) and P-values associated with real time-quantitative PCR (RT-qPCR) analysis of interferon stimulated genes (ISGs) in bovine endometrial epithelial and stroma fibroblast (SF) cells treated with medium alone (Control) or medium containing recombinant ovine IFNT (100 ng/mL; 300 μL total volume; 30 ng equivalent) for 6 h during 3D culture. Relative expression data are normalized over the geometric mean of reference genes, *RNF11* and *SDHA*. Data are presented as LSM ± SEM.

Gene	Endometrial Cell Type	Control	IFNT	P-value
OAS2	Epithelial	0.59 ± 1.06	9.97 ± 1.22	< 0.01
	Fibroblast	0.25 ± 0.13	1.62 ± 0.15	< 0.01
STAT1	Epithelial	0.92 ± 0.74	2.84 ± 0.86	NS
	Fibroblast	0.99 ± 0.31	1.66 ± 0.36	NS
BATF2	Epithelial	0.59 ± 1.03	8.51 ± 1.19	< 0.001
	Fibroblast	0.30 ± 0.25	1.55 ± 0.29	< 0.01
IDO1	Epithelial	1.69 ± 0.33	1.82 ± 0.38	NS
	Fibroblast	0.48 ± 0.16	0.93 ± 0.18	NS
MAP6	Epithelial	1.86 ± 0.30	1.16 ± 0.35	NS
	Fibroblast	0.61 ± 0.24	0.97 ± 0.27	NS
TNFSF13B	Epithelial	0.48 ± 0.80	12.70 ± 0.93	< 0.001
	Fibroblast	0.33 ± 0.35	1.48 ± 0.41	< 0.05
LGALS9	Epithelial	3.07 ± 2.99	36.78 ± 3.45	< 0.001
	Fibroblast	0.04 ± 0.15	0.79 ± 0.18	< 0.01

Figure 1. Isolated bovine endometrial cell monocultures and the endometrial 3D cell culture system. (A and B) Monocultures of purified bovine endometrial epithelial (A) and stroma fibroblast (SF) (B) cells were stained for vimentin (red) and cytokeratin (green), an epithelial cell protein, using a dual immunocytochemical (ICC) technique. Nuclei were also stained with Hoechst (blue). Images of ICC and Hoechst staining were then overlaid. (C) 3D bovine endometrial cell cultures of endometrial epithelial and SF cells were treated apically for 6 h with medium alone (Control), medium containing Day 14 pregnant ovine uterine flush fluid (UFF) (1:1; 300 μL total volume) or medium containing recombinant ovine IFNT (100 ng/mL; 300 μL total volume; 30 ng equivalent). In an effort to see epithelial cells in 3D culture, a trans-well insert membrane was removed, sectioned, and stained with hematoxylin and eosin. Round, darkly stained, structures are epithelial cell nuclei.

Figure 2. Real time-quantitative PCR (RT-qPCR) normalized relative quantities (NRQ) for interferon stimulated genes (*ISG15* [A and B] and *LGALS3BP* [C and D]) and pregnancy related genes (*CXCR4* [E and F] and *LIF* [H and I]) in bovine endometrial epithelial and stroma fibroblast cells treated with medium alone (Control) or medium containing Day 14 pregnant ovine uterine flush fluid (UFF) (1:1; 300 μL total volume) for 6 h during 3D culture. Compared to Control 3D cultures (treatment medium only), treating 3D cultures with pregnant ovine UFF increased expression of *ISG15* (A and B) and *LGALS3BP* (C and D) in both the epithelial and stroma fibroblast cells. Expression of *CXCR4* (E) and *LIF* (H) increased only within the epithelial cells. Relative expression data are normalized over the geometric mean of reference genes *PPIA* and *SDHA*. Data are presented as LSM ± SEM. ***P < 0.001, **P < 0.01, *P < 0.05 and NS = non-significant.

Figure 3. Venn diagram (Venny 2.1 BioinfoGP) comparing DEGs identified by RNA-Seq in bovine endometrial epithelial (IFNT dependent epithelial DEGs; Td-Epi DEGs) and stroma fibroblast (SF) (IFNT dependent SF DEGs; Td-SF DEGs) cells treated with recombinant ovine IFNT during 3D culture ($P \leq 0.001$; FDR $P \leq 0.05$). 663 and 80 Td-Epi and Td-SF DEGs, respectively, were identified by RNA-Seq. 584 DEGs were specific to the epithelial cells (Region I), a single gene, *ZC3HAV1*, was specific to the SF cells (Region III) and 79 DEGs were shared between both groups (Region II). Down-regulated DEGs (41) were only detected within the epithelial cells and within Region I. Tables below include the NCBI gene ID, symbol, and expression LogFC values of the top 10 most up-regulated DEGs in the Td-Epi and Td-SF groups as well as the top 10 most down-regulated DEGs in the Td-Epi group. ($P \leq 0.001$; FDR $P \leq 0.05$)

Figure 4. Venn diagram (Venny 2.1 BioinfoGP) comparing DEGs identified by RNA-Seq in mid-luteal phase bovine endometrium treated with Day 15 bovine conceptuses and recombinant ovine IFNT (bovine conceptus induced, IFNT dependent endometrial DEGs; CiTd-Endo DEGs; Mathew et al. [30]) with DEGs identified by RNA-Seq in bovine endometrial epithelial (IFNT dependent epithelial DEGs; Td-Epi DEGs) and stroma fibroblast (SF) (IFNT dependent SF DEGs; Td-SF DEGs) cells treated with recombinant ovine IFNT during 3D culture. 224 DEGs in the Td-Epi and Td-SF groups (Regions I, II and III) overlapped with 369 CiTd-Endo DEGs. In both studies, the 224 DEGs were up-regulated. 154 DEGs (Region I) were specific to the epithelia cells while a single transcript, *ZC3HAV1*, was exclusive to the SF cells (Region III). 69 DEGs (Region II) were shared between both cell types.

Figure 5. (A-J) Real time-quantitative PCR (RT-qPCR) normalized relative quantities (NRQ) for interferon stimulated genes *ISG15* (A and B), *MX1* (C and D), *MX2* (E and F), *LGALS3BP* (G and H) *and ZC3HAV1* (I and J) in bovine endometrial epithelial and stroma fibroblast cells treated with medium alone (Control) or medium containing recombinant ovine IFNT (100 ng/mL; 300 μL total volume; 30 ng equivalent) for 6 h during 3D culture. Compared to Control 3D cultures, treating 3D cultures with IFNT increased expression of *ISG15, MX1, MX2, and LGALS3BP* in both the epithelial (A, C, E, G, and I) and stroma fibroblast cells (B, D, F, H, and J). Expression of *ZC3HAV1* increased within the stroma fibroblast cells (J) but not epithelial cells (I) despite applying IFNT apically to 3D cultures. Relative expression data are normalized over the geometric mean of reference genes *RNF11* and *SDHA*. Data are presented as LSM ± SEM. ***P < 0.001, **P < 0.01, *P < 0.05 and NS = non-significant.

Figure 1.

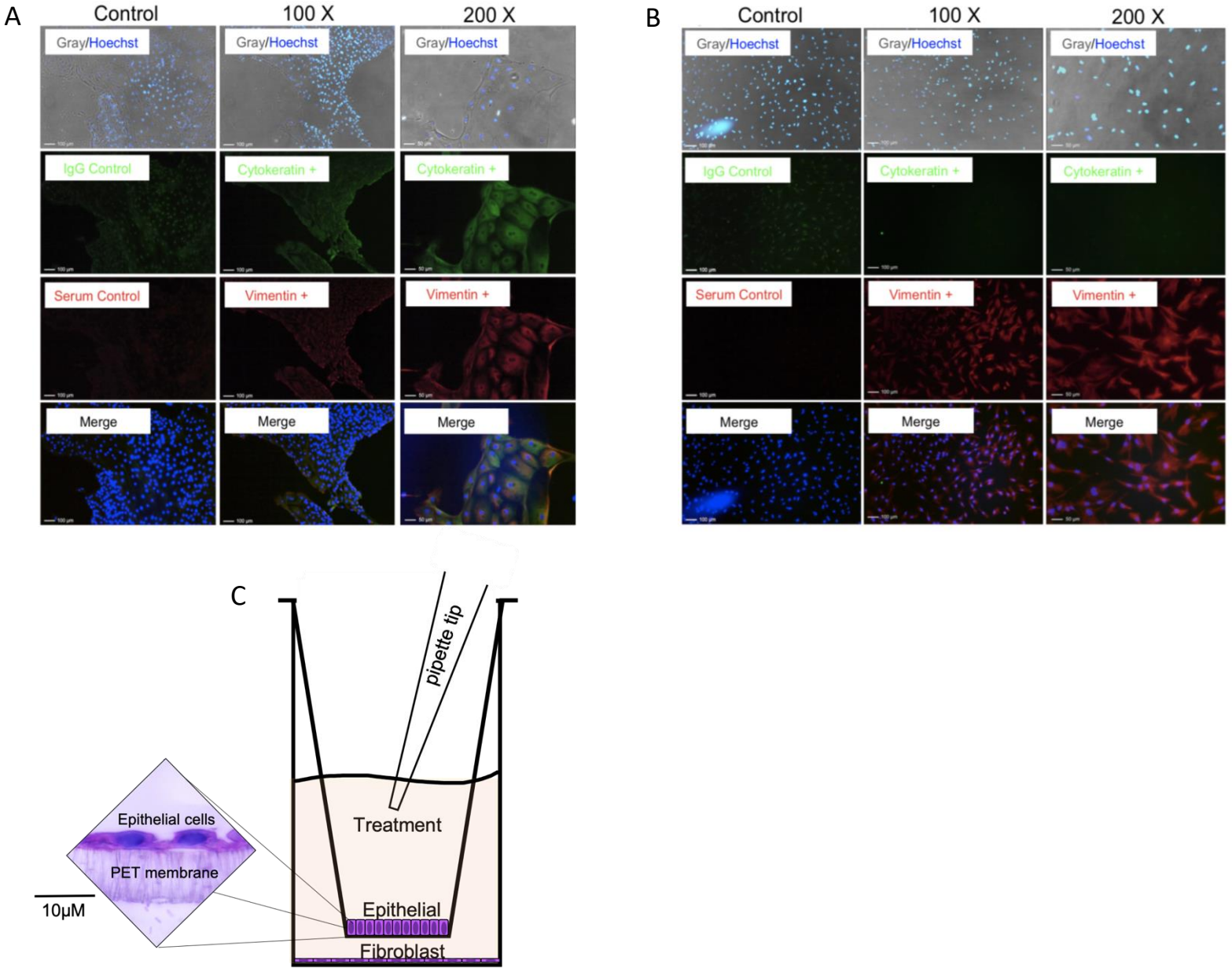
A
Control
100 X
200 X
Gray/Hoechst
IgG Control
Cytokeratin +
Serum Control
Vimentin +
Merge
B
C
pipette tip
Treatment
Epithelial cells
PET membrane
10μM
Epithelial
Fibroblast

Figure 2.

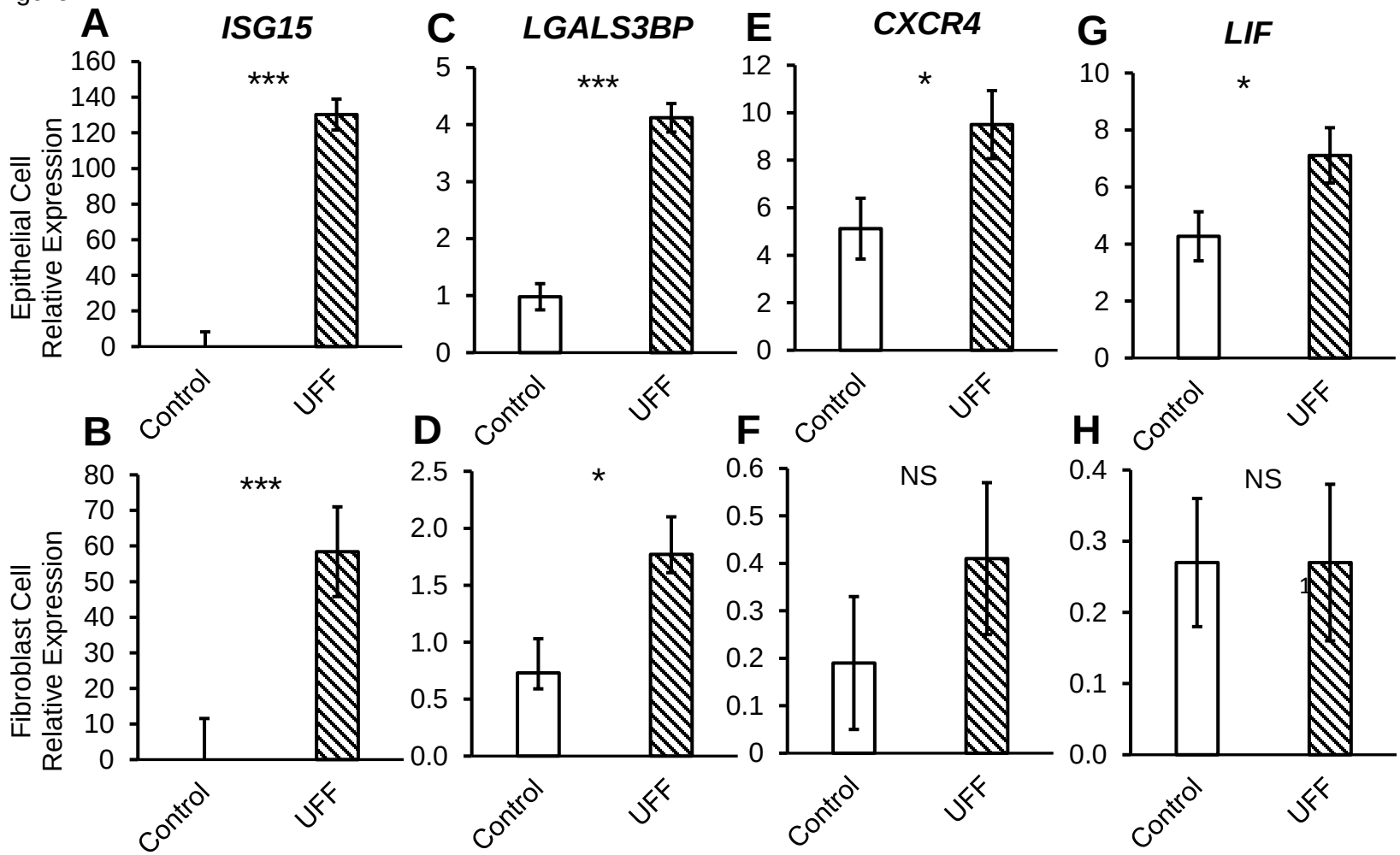
A
ISG15
***
C
LGALS3BP
***
E
CXCR4
*
G
LIF
*
B
***
D
*
F
NS
H
NS
Epithelial Cell
Relative Expression
Fibroblast Cell
Relative Expression
Control
UFF

Figure 3.

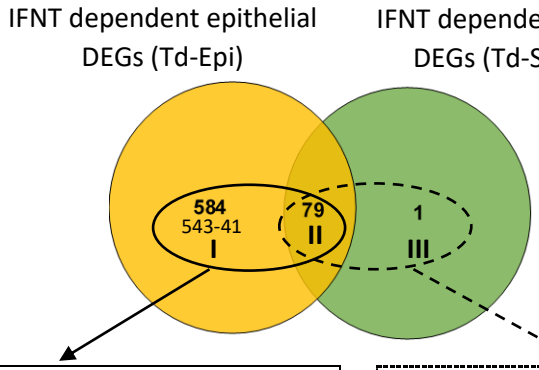

NCBI ID	Gene Symbol	Td-Epi LogFC
522469	BATF2	11.88
280873	MX2	10.26
508348	IFI44	9.95
100139670	IFIT1	9.65
529660	OAS2	9.51
281702	CNGB1	9.15
767910	PLAC8	8.96
538771	KIF5C	8.66
505308	SAA4	8.51
508333	ZBP1	8.47
518159	FITM2	-1.02
532560	SLC25A15	-1.04
789710	KLF13	-1.11
534933	SCRN1	-1.16
614070	FAM92A	-1.43
104974273	GVQW3	-2.00
100847156	LOC100847156	-2.08
528799	ZMYND10	-2.78
616819	LOC616819	-5.45
518794	MAP6	-6.50

NCBI ID	Gene Symbol	Td-SF LogFC
529660	OAS2	9.63
508347	IFI44L	8.66
506415	RSAD2	8.35
508333	ZBP1	8.06
654488	OAS1Y	7.95
280873	MX2	7.83
280872	MX1	7.77
767910	PLAC8	7.75
508348	IFI44	7.63
507215	TNFSF10	7.50

Figure 4.

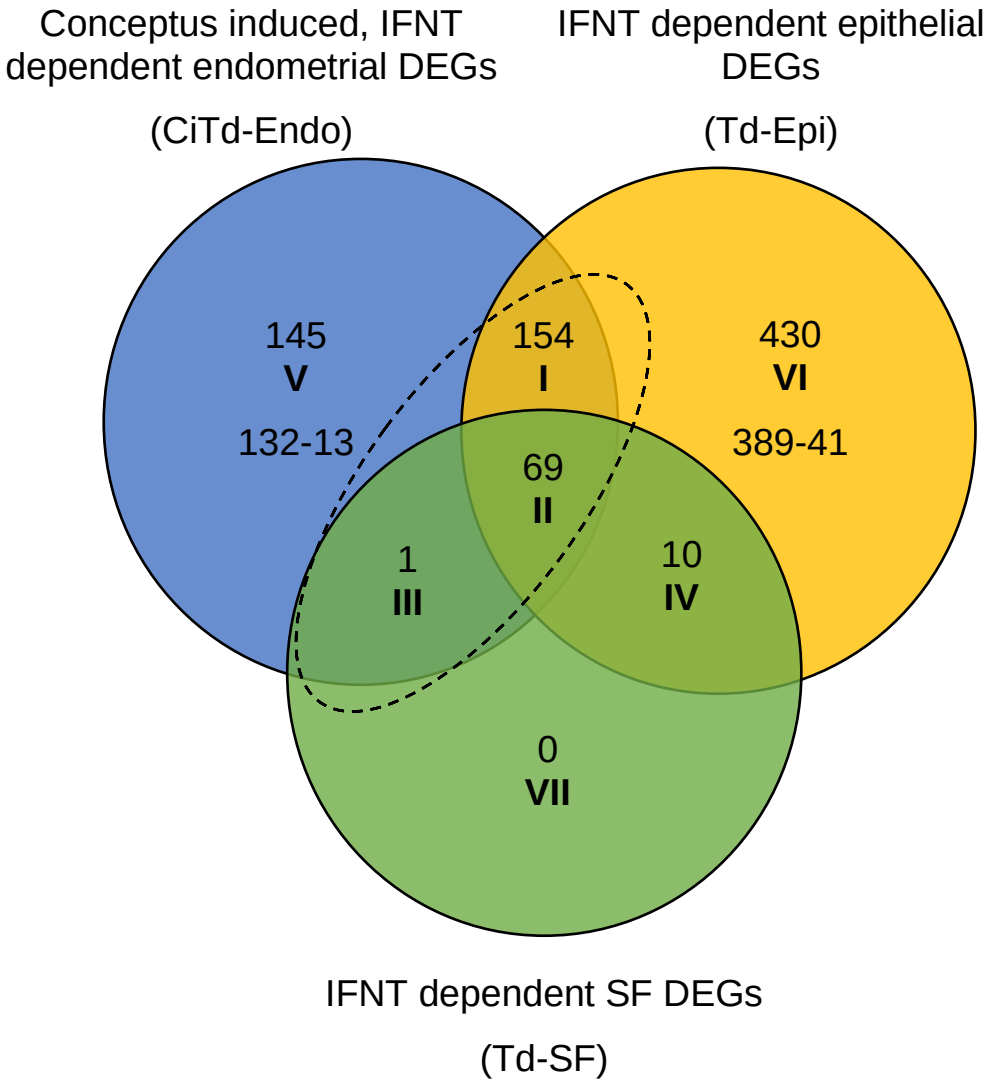
Conceptus induced, IFNT dependent endometrial DEGs
(CiTd-Endo)
IFNT dependent epithelial DEGs
(Td-Epi)
145
V
132-13
154
I
69
II
430
VI
389-41
1
III
10
IV
0
VII
IFNT dependent SF DEGs
(Td-SF)

Figure 5.

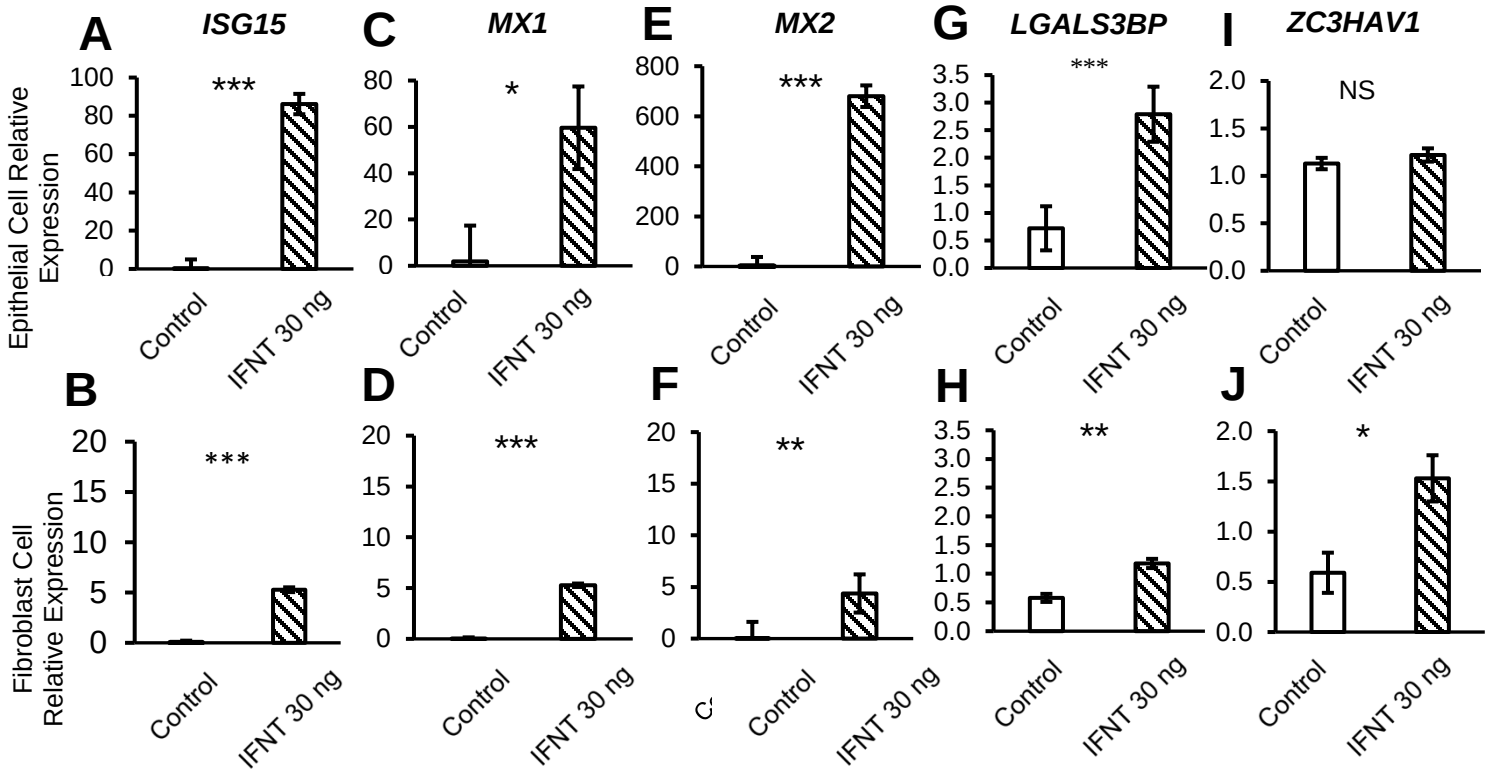
A
ISG15
C
MX1
E
MX2
G
LGALS3BP
I
ZC3HAV1
Epithelial Cell Relative Expression
B
D
F
H
J
Fibroblast Cell Relative Expression
***
*
***
***
NS
***
**
**
*
Control
IFNT 30 ng